Relationship among Redox Potentials, Proton Dissociation Constants of Pyrrolic Nitrogens, and in Vivo and in Vitro Superoxide Dismutating Activities of Manganese(III) and Iron(III) Water-Soluble Porphyrins

Ines Batinić-Haberle,[†] Ivan Spasojević,[‡] Peter Hambright,[§] Ludmil Benov,[†,||] Alvin L. Crumbliss,[‡] and Irwin Fridovich*[,†]

Department of Biochemistry, Duke University Medical Center, Durham, North Carolina 27710, Department of Chemistry, Duke University, Durham, North Carolina 27708, and Department of Chemistry, Howard University, Washington, D.C. 20059

Received January 28, 1999

The log k_{cat} values for the dismutation of $O_2^{\bullet-}$ by a series of monohydroxoiron(III) and aquamanganese(III) porphyrins, including ortho, meta, and para isomers of 5,10,15,20-tetrakis(*N*-alkylpyridiniumyl)porphyrins, were found to vary linearly with the metal-centered redox potentials ($E_{1/2}$) for the M(III)/M(II) couple. Each 120 mV increase in $E_{1/2}$ imparted a 10-fold increase in k_{cat}. The observed behavior is in accord with the Marcus equation for outer-sphere electron-transfer reactions, suggesting that the same mechanism is operative for iron and manganese porphyrins. The Marcus plot enabled us to estimate the self-exchange rate constants of monohydroxoiron porphyrins to be ∼1 order of magnitude higher than those of aquamanganese porphyrins. Furthermore, $E_{1/2}$ values for all of the metalloporhyrins investigated were linearly related to the acid dissociation constants (pK_{a3}) of the pyrrolic nitrogen of the metal-free porphyrins, indicating that either $E_{1/2}$, or the more readily measured pK_{a3}, may be useful in predicting SOD activity in vitro. The most potent compounds investigated, with respect to SOD activity, are those of the ortho *N*-alkylpyridiniumyl series. Ortho *N*-alkylpyridiniumyl groups are more electron withdrawing than are the meta or para groups, thus imparting a more positive redox potential and a correspondingly higher SOD activity. Sufficiently positive potentials, or sufficiently low pK_{a3} values, are necessary for useful SOD activity, but so is the absence of toxicity. Despite their favorable redox potentials and SOD activities, all Fe(III) porphyrins investigated were toxic to *Escherichia coli* under both aerobic and anaerobic conditions and to both SOD-deficient and SOD-proficient strains. Only the ortho and meta manganese isomers of the *N*-alkylpyridiniumyl series (Mn^{III}-TE-2-PyP^{5+}, Mn^{III}TM-2-PyP^{5+} and Mn^{III}TM-3-PyP^{5+}) significantly protected SOD-deficient *E. coli* and allowed growth in an aerobic minimal medium. In previous work, we established that the lower toxicity of these compounds is due to diminished ability to bind to nucleic acids. The Mn(III) complexes are preferable to the Fe(III) complexes for SOD mimics possibly due to a lower tendency for axial ligation. We propose $E_{1/2} \geq +0.05$ V vs NHE and/or $pK_{a3} \leq 2.0$ as necessary requirements for Mn porphyrins to be considered useful SOD mimics.

Introduction

Metalloporphyrins are being explored for use as photosensitizers[1,2] and for treating pathologies in which the superoxide radical and its progeny are suspected of playing important roles.[3−10] To optimize such applications, more information about the chemistry and biochemistry of water-soluble porphyrins is needed.[11] Cationic porphyrins in particular are being investigated as catalysts for the dismutation of $O_2^{\bullet-}$,[5,6,12−16] for the isomerization of peroxynitrite[3−5] and as inhibitors of lipid peroxidation.[15] Until recently, work with *N*-methylpyridiniumyl-substituted metalloporphyrins was concentrated on the para

* To whom the correspondence should be addressed.
[†] Duke University Medical Center.
[‡] Duke University.
[§] Howard University.
[||] Present address: Department of Biochemistry, Kuwait University Faculty of Medicine.

(1) Dolphin, D. *Can. J. Chem.* **1994**, *72*, 1005.
(2) Bonnett, R. *Chem. Soc. Rev.* **1995**, *24*, 19.
(3) Misko, T. P.; Highkin, M. K.; Veenhuizen, A. M.; Manning, P. T.; Stern, M. K.; Currie, M. G.; Salvemini, D. *J. Biol. Chem.* **1998**, *273*, 15646.
(4) Salvemini, D.; Wang, Z.-Q.; Stern, M. K.; Currie, M. G.; Misko, T. P. *Proc. Natl. Acad. Sci. U.S.A.* **1998**, *95*, 2659.
(5) Lee, J.; Hunt, J. A.; Groves, J. T. *J. Am. Chem. Soc.* **1998**, *120*, 6053.
(6) Ferrer-Sueta, G.,; Batinić-Haberle, I.; Spasojević, I.; Fridovich, I.; Radi, R. *Chem. Res. Toxicol.* **1999**, *12*, 442.
(7) Ding, L.; Balzarini, J.; Schols, D.; Meunier, B.; De Clercq, E. *Biochem. Pharmacol.* **1992**, *44*, 1675.
(8) Pasternack, R. F.; Gibbs, E. J.; Villafranca, J. J. *Biochemistry* **1983**, *22*, 5409.
(9) Min, L.; Guo, Q.; Pasternack, R. F.; Wink, D. J.; Seeman, N. C.; Kallenbach, N. R. *Biochemistry* **1990**, *29*, 1614.
(10) Pasternack, R. F.; Gibbs, E. J.; Gaudemer, A.; Antebi, A.; Bassner, S.; De Poy, L.; Turner, D. H.; Williams, A.; Laplace, F.; Lansard, M. H.; Merienne, C.; Perrée-Fauvet, M. *J. Am. Chem. Soc.* **1985**, *107*, 8179.
(11) Meng, G. G.; James, B. R.; Skov, K. A.; Korbelik, M. *Can. J. Chem.* **1994**, *72*, 2447.
(12) Batinić-Haberle, I.; Liochev, S. I.; Spasojević, I.; Fridovich, I. *Arch. Biochem. Biophys.* **1997**, *343*, 225.
(13) (a) Batinić-Haberle, I.; Benov, L.; Spasojević, I.; Fridovich, I. *J. Biol. Chem.* **1998**, *273*, 24521. (b) Batinić-Haberle, I.; Stevens, R. D.; Fridovich, I. *J. Porphyrins Phthalocyanines*, in press.
(14) Kachadourian, R.; Batinić-Haberle, I.; Fridovich, I. *Inorg. Chem.***1999**, *38*, 391.
(15) (a) Day, B. J.; Batinić-Haberle, I.; Crapo, J. D. *Free Radic. Biol. Med.* **1998**, *26*, 730. (b) Bloodsworth, A.; O'Donnell, V.; Batinić-Haberle, I.; Chumley, P. H.; Day, B. J.; Crow, J. P.; Crapo, J.; Duncan, C. Submitted for publication in *Biochemistry*.
(16) Lee, J.; Hunt, J. A.; Groves, J. T. *J. Am. Chem. Soc.* **1998**, *120*, 7493.

10.1021/ic990118k CCC: $18.00
Published on Web 08/17/1999

compounds,[3−5,12] and the advantages offered by the ortho isomer have only recently been appreciated.[6,13−15] The advantages of the ortho compound are due to a higher metal-centered redox potential, which imparts greater catalytic activity, and to the axial orientation of the *N*-alkylpyridiniumyl groups with respect to the porphyrin plane, which diminishes interaction with DNA.[13a]

We now compare the Mn(III) and Fe(III) complexes of meso-substituted ortho, meta, and para tetrakis(*N*-alkylpyridiniumyl)-porphyrins with regard to their activity as catalysts for the dismutation of $O_2^{\bullet-}$ and as agents for the protection of SOD-deficient *E. coli* against endogenous $O_2^{\bullet-}$. We explore the relationship among the rate constants for catalysis of $O_2^{\bullet-}$ dismutation (log $k_{cat}(O_2^{\bullet-})$), the metal-centered redox potentials ($E_{1/2}$) of the M(III)/M(II) couple, and the proton dissociation constants of the pyrrolic nitrogens (pK_{a3}). To establish whether this interdependence might be widely applied to any water-soluble metalloporphyrin, and thus present a valuable diagnostic tool, we have extended our study to a series of anionic and cationic iron and manganese porphyrins.

Materials and Methods

General Reagents. $MnCl_2 \cdot 4H_2O$, $ZnCl_2$ and Baker-flex silica gel IB were purchased from J. T. Baker. $FeCl_2 \cdot 4H_2O$, *N,N′*-dimethylformamide (DMF), ethyl *p*-toluenesulfonate (ETS), 2-propanol (99.5+%), NH_4PF_6 (99.99%), $K_3Fe(CN)_6$, NaCl, 1-methylimidazole (1-MeIm), D-mannitol, and tetrabutylammonium chloride were from Sigma-Aldrich, while xanthine and ferricytochrome *c* were purchased from Sigma. Caution has to be taken when using ferricytochrome *c*, since significant variations among different lots were observed. Methanol (anhydrous, absolute), ethanol (absolute), acetone, ethyl ether (anhydrous), KNO_3, hydrochloric acid, phosphate salts, EDTA, glucose, inorganic salts, and KOH were from Mallinckrodt, casamino acids were from Difco, and acetonitrile was from Fisher Scientific. Xanthine oxidase was prepared by R. D. Wiley and was supplied by K. V. Rajagopalan.[17] Catalase was from Boehringer. Ultrapure argon was from National Welders Supply Co., and Wako-gel silica gel, C300, was from Wako Chemicals.

Porphyrins of the *N*-Alkypyridiniumyl Series. H_2T-2-PyP, and H_2TM-2(3)-PyP^{4+} (**2**, **3**) (Chart 1) and Fe^{III}TM-4-PyP^{5+} (**4$_{Fe}$**) in the form of their chloride salts were obtained from Mid-Century Chemicals, Chicago, IL. The *N*-ethylated analogue H_2TE-2-PyP^{4+} (**1**) was prepared by *N*-ethylation of 500 mg of H_2T-2-PyP with 20 mL of ethyl *p*-toluenesulfonate in 100 mL of DMF for 24 h at ∼100 °C. The course of *N*-ethylation was followed by thin-layer chromatography on Baker-flex silica gel IIB, using KNO_3-saturated H_2O/H_2O/acetonitrile (1:1:8). Upon completion, 200 mL each of water and chloroform were added to the reaction mixture in a separatory funnel and shaken well. The chloroform layer was discarded, and the extraction with $CHCl_3$ was repeated several times. The aqueous layer was filtered, and the porphyrin was precipitated as the PF_6^- salt by the addition of a concentrated aqueous solution of NH_4PF_6. The precipitate was thoroughly washed with 2-propanol/diethyl ether (1:1) and dried briefly in vacuo. It was then dissolved in acetone, followed by filtration and precipitation as the chloride salt with tetrabutylammonium chloride. The precipitate was washed thoroughly with acetone and dried in vacuo at room temperature. H_2TE-2-PyP^{4+} (**1**) was characterized as follows. UV/vis spectroscopy: λ_{max}, nm (log ϵ) = 414.0 (5.33), 659.1 (3.28), 634.9 (3.38), 582.2 (3.80), 545.4 (3.58), 511.2 (4.20). TLC: Aldrich silica gel on glass plates (Z12268-8), $R_f = 0.11$; and Bakerflex silica gel IB, $R_f = 0.18$ (with KNO_3-saturated H_2O/H_2O/acetonitrile (1:1:8)). Anal. Calcd for H_2TE-2-PyPCl$_4 \cdot 3.5H_2O$ ($C_{48}H_{53}N_8O_{3.5}Cl_4$): C, 61.34; H, 5.68; N, 11.92; Cl, 15.09. Found: C, 61.13; H, 5.77; N, 11.86; Cl, 15.38.

Metalloporphyrins of the *N*-Alkylpyridiniumyl Series. The data for Mn^{III}TM-2(3,4)-PyP^{5+} (**2$_{Mn}$**, **3$_{Mn}$**, **4$_{Mn}$**) were used as given in ref 13a. The insertion of manganese into H_2TE-2-PyP^{4+} was done in the same way as in the preparation of Mn^{III}TM-2-PyP^{5+}.[13,14] Molar absorptivity of the ortho isomer Mn^{III}TE-2-PyP^{5+} (**1$_{Mn}$**): log $\epsilon_{453.8}$ = 5.14. TLC: $R_f = 0.053$ (Aldrich silica plates) and $R_f = 0.09$ (Bakerflex silica plates) with KNO_3-saturated H_2O/H_2O/acetonitrile (1:1:8). Anal. Calcd for Mn^{III}TE-2-PyPCl$_5 \cdot 4H_2O$ ($MnC_{48}H_{52}N_8O_4Cl_5$): C, 55.37; H, 5.03; N, 10.76. Found: C, 55.32; H, 5.14; N, 10.73.

The insertions of iron into H_2TM-2(3)-PyP^{4+} and H_2TE-2-PyP^{4+} were performed in aqueous acidic (0.01 M HCl) solutions with a 20-fold excess of $FeCl_2 \cdot 4H_2O$, under refluxing conditions for 24 and 48 h, respectively.[18] Removal of the excess metal and the isolation of the chloride salt were accomplished as already described for the manganese analogues. The UV/vis spectral data obtained in 0.01 M HCl were in agreement with literature data: log $\epsilon_{393.6}$ = 5.11 (Fe^{III}TM-2-PyP^{5+} (**2$_{Fe}$**));[19] log $\epsilon_{397.4}$ = 5.01 (Fe^{III}TM-4-PyP^{5+} (**4$_{Fe}$**)).[20] The molar absorptivity of Fe^{III}TM-3-PyP^{5+} (**3$_{Fe}$**) in 0.01 M HCl was measured to be log $\epsilon_{397.8}$ = 5.01. Anal. Calcd for the ortho isomer, Fe^{III}TM-2-PyPCl$_5 \cdot 5H_2O$ ($FeC_{44}H_{46}N_8O_5Cl_5$): C, 52.84; H, 4.64; N, 11.20; Cl, 17.73. Found: C, 52.78; H, 4.58; N, 11.49; Cl, 17.60. Calcd for the meta isomer, FeT^{III}M-3-PyPCl$_5 \cdot 6H_2O$ ($FeC_{44}H_{48}N_8O_6Cl_5$): C, 51.91; H, 4.75; N, 11.00; Cl, 17.41. Found: C, 51.94; H, 4.78; N, 11.11; Cl, 17.38. Calcd for the para isomer, Fe^{III}TM-4-PyPCl$_5 \cdot 5H_2O$ ($FeC_{44}H_{46}N_8O_5Cl_5$): C, 52.84; H, 4.64; N, 11.20; Cl, 17.73. Found: C, 52.81; H, 4.72; N, 11.26; Cl, 17.58. The purity of Fe^{III}TE-2-PyPCl$_5$ was assumed on the basis of the analysis of the metal-free ligand given above. The molar absorptivity of the Soret band of Fe^{III}TE-2-PyP^{5+} (**1$_{Fe}$**) was taken to be log $\epsilon_{396.8}$ = 5.16, on the basis of the similarities of the molar absorptivities of *N*-methylated and *N*-ethylated Mn analogues.[13a,14]

It was previously shown[13a] that all isomers of Mn^{III}TMPyP^{5+}, at 6 μM, are stable toward metal removal in 36% HCl for at least 24 h. The same was true for Mn^{III}TE-2-PyP^{5+} and for Fe^{III}TM(E)-2(3,4)-PyP^{5+}.

Partially Methylated MnT-2-PyP$^+$. In addition to fully *N*-methylated Mn^{III}TM-2-PyP^{5+}, di- and tri-*N*-methylated derivatives were examined for their metal-centered redox potentials and SOD activities. The *N*-methylation, followed by thin-layer chromatography, was stopped when the mono-*N*-methylated compound disappeared from the reaction mixture. The solid mixture of the compounds of different degrees of *N*-methylation, in the forms of their chloride salts, was prepared in the same way as H_2TMPyP^{4+} or Mn^{III}TMPyP^{5+}. Its aqueous solution was placed on a Wako-gel silica gel C300 column and cleanly separated into di- (Mn^{III}BM-2-PyP^{3+}) (**2a$_{Mn}$**), tri- (Mn^{III}TrM-2-PyP^{4+}) (**2b$_{Mn}$**), and tetra-*N*-methylated species (**2$_{Mn}$**). Elution was performed with KNO_3-saturated H_2O/H_2O/acetonitrile (1:1:8). The same method of separation was applied to the mixture of differently *N*-methylated metal-free ligands. All the metal-free ligands (di-, tri-, and tetra-*N*-methylated) have a Soret band at the same wavelength, λ = 413.2 nm. We made the assumption, therefore, that the molar absorptivities of the partially methylated compounds were about the same as that of the fully methylated porphyrin, log $\epsilon_{413.2}$ = 5.32. Upon metalation, which was accompanied by a set of isosbestic points, no observable differences in the final absorptions among the manganese complexes of di-, tri-, and tetra-*N*-methylated ligands were detected at the wavelengths of the metalloporphyrin Soret bands, 458.4, 456.4, and 453.4 nm, respectively. Therefore, the same molar absorptivity of log ϵ = 5.11 was used to determine the concentrations of these manganese porphyrins.

Other Metalloporphyrins. Fe^{III}T(TMA)P^{5+} (**5$_{Fe}$**), Fe^{III}T(TFTMA)-P^{5+} (**8$_{Fe}$**), Fe^{III}TCPP^{3-} (**9$_{Fe}$**), Fe^{III}TSPP^{3-} (**10$_{Fe}$**), Fe^{III}T(2,6-Cl$_2$-3-SO$_3$-P)P^{3-} (**11$_{Fe}$**), Fe^{III}T(2,4,6-Me$_3$-3,5-(SO$_3$)$_2$-P)P;$^{7-}$ (**12$_{Fe}$**), Mn^{III}T(TMA)-P^{5+} (**5$_{Mn}$**), Mn^{III}PTrM-2-PyP^{4+} (**6$_{Mn}$**), Mn^{III}T(α,α,α,α-2-MINP)P^{5+} (**7$_{Mn}$**), Mn^{III}T(TFTMA)P^{5+} (**8$_{Mn}$**), Mn^{III}TCPP^{3-} (**9$_{Mn}$**), Mn^{III}TSPP^{3-} (**10$_{Mn}$**), Mn^{III}T(2,6-Cl$_2$-3-SO$_3$-P)P^{3-} (**11$_{Mn}$**), Mn^{III}T(2,4,6-Me$_3$-3,5-

(17) Waud, W. R.; Brady, F. O.; Wiley, R. D.; Rajagopalan, K. V. *Arch. Biochem. Biophys.* **1975**, *19*, 695.

(18) Hambright, P.; Gore, T.; Burton, M. *Inorg. Chem.* **1976**, *15*, 2314.

(19) (a) Chen, S.-M.; Sun, P.-J.; Su, Y. O. J. *Electroanal. Chem. Interfacial Electrochem.* **1990**, *294*, 151. (b) Rodgers, K. R.; Reed, R. A.; Su, Y. O.; Spiro, T. G. *Inorg. Chem.* **1992**, *31*, 2688.

(20) Forshey, P. A.; Kuwana, T. *Inorg. Chem.* **1981**, *20*, 693.

Chart 1. The Porphyrin Ligands Studied

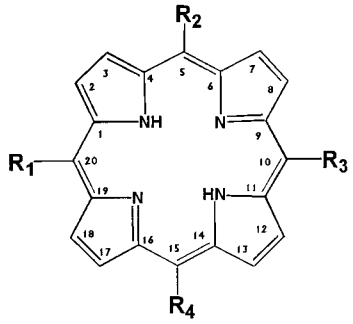

***meso*-pyridyl series:**

1 $H_2TE\text{-}2\text{-}PyP^{4+}$ $R_1=R_2=R_3=R_4=$ 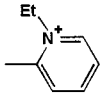

2 $H_2TM\text{-}2\text{-}PyP^{4+}$ $R_1=R_2=R_3=R_4=$ 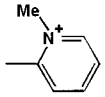

3 $H_2TM\text{-}3\text{-}PyP^{4+}$ $R_1=R_2=R_3=R_4=$ 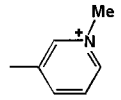

4 $H_2TM\text{-}4\text{-}PyP^{4+}$ $R_1=R_2=R_3=R_4=$ 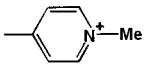

2a $H_2BM\text{-}2\text{-}PyP^{2+}$ $R_1=R_2=$ 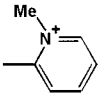

$R_3=R_4=$ 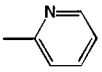

2b $H_2TrM\text{-}2\text{-}PyP^{3+}$ $R_1=R_2=R_3=$ 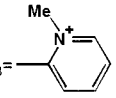

$R_4=$ 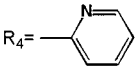

***meso*-phenyl series:** 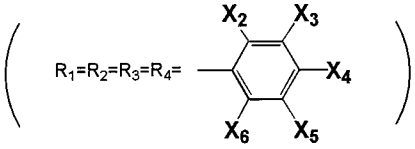

hematoporphyrin IX:

14 $H_2hematoP^{2-}$

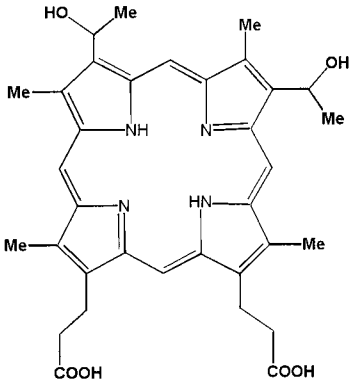

5 $H_2T(TMA)P^{4+}$ $X_2=X_3=X_5=X_6=$ H

$X_4=$ 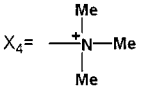

8 $H_2T(TFTMA)P^{4+}$ $X_2=X_3=X_5=X_6=$ F

$X_4=$ 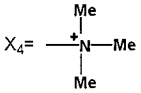

11 $H_2T(2,6\text{-}Cl_2\text{-}3\text{-}SO_3\text{-}P)P^{4-}$ $X_4=X_5=$ H; $X_2=X_6=$ Cl; $X_3=$ SO_3^-

6 $H_2PTrM\text{-}2\text{-}PyP^{3+}$ $R_1=R_2=R_3=$ 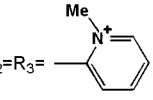

$R_4=$ 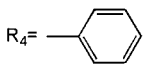

9 H_2TCPP^{4-} $X_2=X_3=X_5=X_6=$ H; $X_4=$ COO^-

12 $H_2T(2,4,6\text{-}Me_3\text{-}3,5\text{-}(SO_3)_2\text{-}P)P^{8-}$ $X_2=X_4=X_6=$ Me; $X_3=X_5=$ SO_3^-

7 $H_2T(\alpha\alpha\alpha\alpha\text{-}2\text{-}MINP)P^{4+}$ $X_3=X_4=X_5=X_6=$ H

$X_2=$ 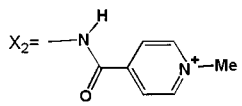

10 H_2TSPP^{4-} $X_2=X_3=X_5=X_6=$ H; $X_4=$ SO_3^-

13 $H_2T(2,6\text{-}F_2\text{-}3\text{-}SO_3\text{-}P)P^{4-}$ $X_4=X_5=$ H; $X_2=X_6=$ F; $X_3=$ SO_3^-

$(SO_3)_2\text{-}P)P^{7-}$ (**12_{Mn}**), $Mn^{III}T(2,6\text{-}F_2\text{-}3\text{-}SO_3\text{-}P)P^{3-}$ (**13_{Mn}**), and $Mn^{III}hematoP^-$ (**14**), were used as obtained from Mid-Century Chemicals, Chicago, IL. $ZnTM\text{-}2\text{-}PyP^{4+}$ was prepared as described for $Mn^{III}TM\text{-}2\text{-}PyP^{5+}$.[13a] All porphyrins investigated are shown in Chart 1.

Proton Dissociation Constants of the Pyrrolic Nitrogens. When available, the pK_{a3} data for eq 1 were taken from the literature.[21−30]

(21) Hambright, P.; Fleischer, E. B. *Inorg. Chem.* **1970**, *9*, 1757.

Table 1. Metal-Centered Redox Potentials (V vs NHE) for the M(III)/M(II) Couples of Iron ($Fe^{III}P(H_2O)$, $Fe^{III}P(OH)$, $Fe^{III}P(1\text{-MeIm})_2$) and Manganese ($Mn^{III}P(H_2O)$) Porphyrins and Proton Dissociation Constants of Pyrrolic Nitrogens, pK_{a3} (Charges Omitted)

porphyrin	$E_{1/2}(Mn^{III}P(H_2O))^a$	$E_{1/2}(Fe^{III}P(H_2O))^b$	$E_{1/2}(Fe^{III}P(OH))^c$	$E_{1/2}(Fe^{III}P(1\text{-MeIm})_2)^d$	pK_{a3}
H_2TE-2-PyP^{4+} (**1**)	+0.228	+0.380	+0.215	+0.440	−0.9[e]
H_2TM-2-PyP^{4+} (**2**)	+0.220	+0.355	+0.212	+0.432	−0.9[f]
H_2PTrM-2-PyP^{3+} (**6**)	+0.108				0.5[g]
H_2TrM-2-PyP^{3+} (**2b**)	+0.118				
H_2TM-4-PyP^{4+} (**4**)	+0.060	+0.197	+0.107	+0.272	1.4[f]
H_2BM-2-PyP^{2+} (**2a**)	+0.053				
H_2TM-3-PyP^{4+} (**3**)	+0.052	+0.260	+0.115	+0.256	1.8[f]
H_2T(α,α,α,α-2-MINP)P^{4+} (**7**)	−0.030				2.2[h]
H_2T(TFTMA)P^{4+} (**8**)	+0.058	+0.236	+0.283		2.2[h]
H_2T(2,6-Cl_2-3-SO_3-P)P^{4-} (**11**)	+0.088	+0.129	+0.094		2.2[i]
H_2T(2,6-F_2-3-SO_3-P)P^{4-} (**13**)	+0.007				2.5[j]
H_2T(2,4,6-Me_3-3,5-$(SO_3)_2$-P)P^{8-} (**12**)	−0.100	+0.109	+0.045		3.2[j]
H_2T(TMAP)P^{4+} (**5**)	−0.100	+0.054	−0.030	+0.100	4.1[k]
H_2TSPP^{4-} (**10**)	−0.160	+0.023		+0.042	4.8[l]
H_2TCPP^{4-} (**9**)	−0.194			+0.028	5.5[m]
H_2hematoP^{2-} (**14**)	−0.230				6.1[n]

[a] Mn center proved insensitive to axial ligation; under all experimental conditions, the $Mn^{III}P(H_2O)$ species (also referred as $Mn^{III}P$) was obtained, which compares to the iron compound $Fe^{III}P(H_2O)$; all $E_{1/2}$ are determined with errors inside ±3 mV. [b] Data obtained at pH 2 (0.01M HCl, 0.1 M NaCl). [c] Data obtained at pH 7.8, 0.05 M phosphate buffer, 0.1 M NaCl, 0.5 mM porphyrin. [d] Data obtained at pH 7.8, 0.05 M phosphate buffer, 0.1 M NaCl, 0.1 M 1-methylimidazole. [e] pK_{a3} estimated to be about the same as pK_{a3} of the methylated analogue on the basis of their other characteristics. [f] Reference 22. [g] This work. [h] Reference 23. [i] Reference 24. [j] Reference 25. [k] Reference 26. [l] References 27 and 28. [m] Reference 29. [n] Reference 30.

$$H_3P^+ \rightleftharpoons H_2P + H^+ \qquad K_{a3} \tag{1}$$

Otherwise, they were determined as described previously.[27] Charges introduced into porphyrin through meso substituents are omitted in eq 1. The constants are listed in Table 1.

Interaction of Iron Porphyrins with 1-Methylimidazole. The stability constants for $Fe^{III}TMPyP^{5+}$ complexes with 1-methylimidazole were determined by spectrophotometric titrations at 25 °C using a Shimadzu UV-2501 PC spectrophotometer. A 15 mL aliquot of the 20 μM porphyrin in 0.05 M phosphate buffer, pH 7.8, 0.1 M NaCl, was titrated with 1.0 mM−1.0 M 1-methylimidazole solutions that were 20 μM in porphyrin.

Electrochemistry. Measurements were performed using a CH Instruments (computer supported) model 600 voltammetric analyzer as described previously.[13a] A three-electrode system in a small-volume cell (0.5−3 mL), with a 3 mm diameter glassy carbon button working electrode (Bioanalytical Systems), an Ag/AgCl reference electrode, and a Pt auxiliary electrode, was used. Solutions containing 0.05 M phosphate buffer, pH 7.8, 0.1 M NaCl, 0.5 mM metalloporphyrin, and (±) 1-methylimidazole (0.01−2 M) were used. In addition, $E_{1/2}$ values of $Mn^{III}TM\text{-}2\text{-}PyP^{5+}$ and $Mn^{III}TM\text{-}3\text{-}PyP^{5+}$ were determined in the pH region 2−12, in 0.1 M NaCl. Also $E_{1/2}$ values of the iron porphyrins in 0.01 M HCl, 0.1 M NaCl were determined. Scan rates were 10−500 mV/s, typically 10 and 100 mV/s. The potentials were standardized against the potassium ferrocyanide/ferricyanide couple.[31]

SOD Activity in Vitro. The xanthine/xanthine oxidase reaction was the source of $O_2^{\bullet-}$, and ferricytochrome *c* was used as the indicating scavenger for $O_2^{\bullet-}$.[32] The reduction of cytochrome *c* was followed at 550 nm. Assays were conducted in the presence and absence of 0.1 M 1-methylimidazole, in 0.05 M phosphate buffer, pH 7.8, 0.1 mM EDTA, ±15 μg/mL of catalase. The aqueous/acidic (pH 2) iron porphyrins and aqueous manganese stock solutions were assayed. These samples did not measurably perturb the pH of the assay solution. Rate constants for the reaction of metalloporphyrins with $O_2^{\bullet-}$ were based upon competition with 10 μM cytochrome *c*, $k_{cyt} = 2.6 \times 10^5$ M^{-1} s^{-1}.[33] $O_2^{\bullet-}$ was produced at the rate of 1.2 μM/min. Possible interference through inhibition of the xanthine/xanthine oxidase reaction by the test compounds was examined by following the rate of urate accumulation at 295 nm in the absence of cytochrome *c*. No reoxidation of cytochrome *c* by metalloporphyrins was observed. The effect of ionic strength upon the rate constant of dismutation was determined in the region 0.01−0.50 M, adjusted with Na_2SO_4. All measurements were done at 25 °C.

Oxidative Degradation of Porphyrins by H_2O_2. The interaction between H_2O_2 and metal-free porphyrins and metalloporphyrins of the *N*-alkylpyridiniumyl series was followed spectrophotometrically on the Shimadzu spectrophotometer at pH 7.8, 0.1 M NaCl, 0.05 M phosphate buffer, at 25 °C. The porphyrin was kept at 6 μM while [H_2O_2] was varied from 0.5 to 5 mM in the case of $Mn^{III}TMPyP^{5+}$ and from 50 μM to 0.5 mM in the case of $Fe^{III}TMPyP(OH)^{4+}$. $H_2TM\text{-}2\text{-}PyP^{4+}$ and $ZnTM\text{-}2\text{-}PyP^{4+}$ were exposed only to 0.4 M H_2O_2. The oxidative degradation of the compounds, monitored as a decrease in the absorbance of the Soret band of the metalloporphyrin or metal-free ligand, was recorded as a function of time. In addition, rapid scans of spectra were taken on an Applied Photophysics stopped-flow instrument at 25 °C and pH 7.8 (0.05 M phosphate buffer), with 6 μM porphyrin and with 0.2 and 5 mM H_2O_2 in the cases of $Fe^{III}TM\text{-}2\text{-}PyP(OH)^{4+}$ and $Mn^{III}TM\text{-}2\text{-}PyP^{5+}$, respectively.

Effects on *E. coli*. *E. coli* strains AB1157 (wild type) and JI132 (SOD-deficient, s*odA*s*odB*) were obtained from J. A. Imlay.[34] The effect of metalloporphyrins on the growth of these strains was monitored at 700 nm, aerobically and anerobically, in a casamino acid medium (M9CA). Growth was also followed in a minimal medium,[35a] which gives a more stringent test of SOD-like activity.[13a] Deionized water was used throughout. Overnight cultures were treated as previously described,[35b] and the pH of the medium was not perturbed by the addition of aqueous/acidic (pH 2) solutions of iron(III) porphyrins.

(22) Kalayanasundaram, K. *Inorg. Chem.* **1984**, *23*, 2453.
(23) Valiotti, A.; Adeyemo, A.; Williams, R. F. X.; Ricks, L.; North, J.; Hambright, P. *J. Inorg. Nucl. Chem.* **1981**, *43*, 2653.
(24) McClure, J. E.; Baudouin, L.; Mansuy, D.; Marzilli, L. G. *Biopolymers* **1997**, *42*, 203.
(25) Sutter, T. P. G.; Rahimi, R.; Hambright, P.; Bommer, J. C.; Kumar, M.; Neta, P. *J. Chem. Soc., Faraday Trans.* **1993**, *89*, 495.
(26) Krishnamurthy, M. *Indian J. Chem.* **1977**, *15B*, 964.
(27) Sutter, T. P. G.; Hambright, P. *J. Coord. Chem.* **1993**, *30*, 317.
(28) Fleischer, E. B.; Palmer, J. M.; Srivastava, T. S.; Chatterjee, A. *J. Am. Chem. Soc.* **1971**, *93*, 3162.
(29) Pasternack, R. F.; Huber, P. R.; Boyd, P.; Engasser, G.; Francesconi, L.; Gibbs, E.; Fasella, P.; Venturo, G. C.; Hinds, L. deC. *J. Am. Chem. Soc.* **1972**, *94*, 4511.
(30) Hambright, P. *Inorg. Chem.* **1977**, *16*, 2987.
(31) Kolthof, I. M.; Tomsicek, W. J. *J. Phys. Chem.* **1935**, *39*, 945.
(32) McCord, J. M.; Fridovich, I. *J. Biol. Chem.* **1969**, *244*, 6049.
(33) Butler, J.; Koppenol, W. H.; Margoliash, E. *J. Biol. Chem.* **1982**, *257*, 10747.
(34) Imlay, J. A.; Linn, S. *J. Bacteriol.* **1987**, *169*, 2967.
(35) (a) Faulkner, K. M.; Liochev, S. I.; Fridovich, I. *J. Biol. Chem.* **1994**, *269*, 23471. (b) Benov, L.; Fridovich, I. *J. Biol. Chem.* **1998**, *273*, 10313.

Results

Metalloporphyrin/Ligand Equilibria. (a) Interaction of Manganese Porphyrins with 1-Methylimidazole. The absence of low-spin forms of Mn(III) and the weak axial interactions observed here (see below: Electrochemistry of Manganese Porphyrins) and elsewhere[36−39] dominate manganese porphyrin chemistry. The only stability constant available, relating to water-soluble manganese porphyrins, is the one for binding imidazole to $Mn^{III}T(2,6\text{-}Me_2\text{-}3\text{-}SO_3\text{-}P)P^{3-}$, $\log \beta_1 = 2.20$ (lutidine buffer, pH 6.5, 0.1 M $NaClO_4$).[36] On the basis of the ~3 order of magnitude drop in the stability constants for a variety of porphyrin−imidazole complexes, seen upon substituting CH_3 for H on the "aliphatic" nitrogen of imidazole,[40,41] we did not expect any observable ligation of 1-methylimidazole to the manganese metal center.[39]

(b) Interaction of Iron Porphyrins with 1-Methylimidazole. This interaction has already been employed to model the iron center in catalase and peroxidase.[42,43] Here we are interested in modeling the ligation of the iron center by amino acid residues, whereby the SOD-like activity of iron porphyrins may be affected. There is a paucity of data on the stability constants of water-soluble porphyrins with either imidazole or monomethylimidazole. There is also a discrepancy in existing β_2 values for complexes of imidazole with a few water-soluble porphyrins, e.g. 2.5×10^7 M^{-2} [44] and 3×10^5 M^{-2} [45] for Fe^{III}TM-4-PyP^{5+} and 1.4×10^7 M^{-2} [44] and 1.7×10^6 M^{-2} [46] for $Fe^{III}TSPP^{3-}$. Therefore, we undertook the determination of stability constants, β_n, for the 1-methylimidazole complexes of all isomers of $Fe^{III}TMPyP^{5+}$, defined by eq 2. The pK_{a1} values

$$Fe^{III}TMPyP^{5+} + n\ 1\text{-MeIm} \rightleftharpoons Fe^{III}TMPyP(1\text{-MeIm})_n^{5+} \qquad \beta_n \quad (2)$$

(eq 3) of the axially ligated water for the ortho, meta, and para

$$Fe^{III}TMPyP(H_2O)^{5+} \rightleftharpoons Fe^{III}TMPyP(OH)^{4+} + H^+ \qquad K_{a1} \quad (3)$$

isomers are 5.1,[19] 5.9,[47] and 5.5,[48] respectively. The dimerization constants (eq 4) $K_d = 2 \times 10^3$ M^{-1} [48] and $K_d = 2 \times 10^2$ M^{-1}

$$2Fe^{III}P(OH) \rightleftharpoons Fe^{III}P{-}O{-}Fe^{III}P + H_2O \qquad K_d \quad (4)$$

for Fe^{III}TM-4-PyP^{5+} and Fe^{III}TM-2-PyP^{5+} [19] allow us to calculate the monomer concentrations at 20 μM porphyrin to be 96.2% and 99.6%, respectively. The para and meta isomers should have similar dimerization equilibria. Therefore, at pH 7.8 and 20 μM Fe(III) porphyrin, all isomers are present mainly as the monohydroxo species, Fe^{III}TM-2(3,4)-$PyP(OH)^{4+}$. The experimental data obtained from the spectrophotometric titrations of $Fe^{III}TMPyP^{5+}$ isomers by 1-methylimidazole (Figure 1) correspond to eq 5. The fraction of iron porphyrin bound to

$$Fe^{III}TMPyP(OH)^{4+} + n\ 1\text{-MeIm} \rightleftharpoons Fe^{III}TMPyP(1\text{-MeIm})_n^{5+} + OH^- \qquad Q_n \quad (5)$$

imidazole was calculated as $f_c = (A - A_0)/(A_\infty - A_0)$, where A_0 and A_∞ correspond to the absorbances of iron porphyrin and its imidazole complex, respectively.[46] The absorbances were taken

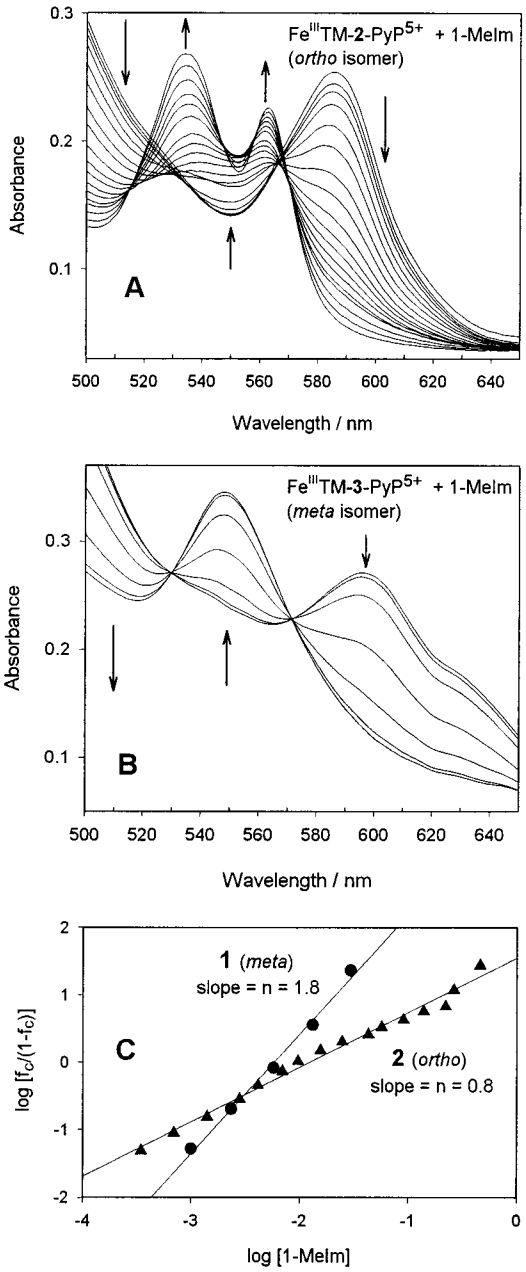

Figure 1. Spectrophotometric titrations of Fe^{III}TM-2-PyP^{5+} (A) and Fe^{III}TM-3-PyP^{5+} (B) with 1-methylimidazole at 20 μM porphyrin concentration, 0.5 mM−0.8 M 1-methylimidazole, 0.1 M NaCl, 0.05 M phosphate buffer, pH 7.8, at 25 °C, and the linear plots $\log(f_c/(1 - f_c))$ vs $\log$ [1-MeIm] (eq 6) (C), whose intercepts define Q_n from eq 5 and whose slopes define the number of imidazoles axially ligated.

(36) Beck, M. J.; Gopinath, E.; Bruice, T. C. *J. Am. Chem. Soc.* **1993**, *115*, 21.
(37) (a) Boucher, L. J. *Coord. Chem. Rev.* **1972**, *7*, 289. (b) Jin, N.; Groves, J. T. *J. Am. Chem. Soc.* **1999**, *121*, 2923.
(38) Neya, S.; Morishima, I.; Yonezawa, T. *Biochemistry* **1981**, *20*, 2610.
(39) Arasasingham, R. D.; Bruice, T. C. *J. Am. Chem. Soc*. **1991**, *113*, 6095.
(40) Walker, F. A.; Simonis, U. Iron Porphyrin Chemistry In *Encyclopedia of Inorganic Chemistry*; King, R. B., Ed.; John Wiley & Sons: New York, 1994; Vol. 4, pp 1785−1846 and references therein.
(41) Walker, F. A.; Lo, M.-W.; Ree, M. T. *J. Am. Chem. Soc*. **1976**, *98*, 5552.
(42) Zipplies, M. F.; Lee, W. A.; Bruice, T. C. *J. Am. Chem. Soc*. **1986**, *108*, 4433.
(43) Balasubramanian, P. N.; Schmidt, E. S.; Bruice, T. C. *J. Am. Chem. Soc.* **1987**, *109*, 7865.
(44) Pasternack, R. F.; Gillies, B. S.; Stahlbush, J. R. *J. Am. Chem. Soc*. **1978**, ***100***, 2613.
(45) Weinraub, D.; Peretz, P.; Faraggi, M. *J. Phys. Chem.* **1982**, *86*, 1839.
(46) Fleischer, E. B.; Fine, D. A. *Inorg. Chim. Acta* **1978**, *29*, 267.
(47) (a) Kobayashi, N. *Inorg. Chem.* **1985**, *24*, 3324. (b) Kobayashi, N.; Koshiyama, M.; Osa, T.; Kuwana, T. *Inorg. Chem.* **1983**, *22*, 3608.
(48) Tondreau, G. A.; Wilkins, R. G. *Inorg. Chem.* **1986**, *25*, 2745.

Table 2. Stability Constants for $Fe^{III}TMPyP^{5+}$ Interactions with 1-Methylimidazole As Defined by Eq 2, Determined at 25 °C

	β_2, M^{-2}	
porphyrin	1-methylimidazole	imidazole
$Fe^{III}TM\text{-}2\text{-}Pyp^{5+}$ (**2_{Fe}**)	$\sim 2 \times 10^7$ [a]	
$Fe^{III}TM\text{-}3\text{-}PyP^{5+}$ (**3_{Fe}**)	7.3×10^5	
$Fe^{III}TM\text{-}4\text{-}PyP^{5+}$ (**4_{Fe}**)	4.6×10^6	2.5×10^7 [b]
		3.0×10^5 [c]
$Fe^{III}TSPP^{3-}$ (**10_{Fe}**)		1.7×10^6 [d]
		1.4×10^7 [b]

[a] $\beta_1 \sim 10^6$ M^{-1}; errors are ±5%. [b] Reference 44. [c] Reference 45. [d] Reference 46.

at 586, 597, and 599 nm for the ortho, meta, and para isomers, respectively. Using $pK_a = 6.95$[49] for 1-methylimidazole, the total imidazole concentration was corrected for the unreactive[46] protonated species. $Q_n/[OH^-]$ was calculated from the intercept of the plot of $\log(f_c/(1 - f_c))$ vs log [1-MeIm] (eq 6), while the slope gives n, the number of imidazoles bound.[46]

$$\log(f_c/(1 - f_c)) = \log(Q_n/[OH]) + n \log [1\text{-MeIm}] \quad (6)$$

For the meta and para isomers of $Fe^{III}TMPyP^{5+}$, $n = 1.8$ and 2.0, respectively (Figure 1C for the meta isomer), which suggests that two imidazoles were bound per complex formed. All spectra for the meta and para isomers passed through a common set of isosbestic points, suggesting the presence of only two porphyrin species during the titration experiment, i.e. high-spin[47] $Fe^{III}TM\text{-}3(4)\text{-}PyP(OH)^{4+}$ and low-spin[47] $Fe^{III}TM\text{-}3(4)\text{-}PyP(1\text{-}MeIm)_2^{5+}$. The absence of evidence for a monoimidazole complex suggests that $K_2 \gg K_1$ (eqs 7 and 8). Thus cooperative

$$Fe^{III}TMPyP^{5+} + 1\text{-MeIm} \rightleftharpoons Fe^{III}TMPyP(1\text{-MeIm})^{5+} \qquad K_1 = \beta_1 \quad (7)$$

$$Fe^{III}TMPyP(1\text{-MeIm})^{5+} + 1\text{-MeIm} \rightleftharpoons Fe^{III}TMPyP(1\text{-MeIm})_2^{5+} \qquad K_2,\ K_2 \cdot K_1 = \beta_2 \quad (8)$$

binding is favored through the high- to low-spin change upon the coordination of the second imidazole. According to eqs 5 and 6 and using Q_2 (since $n = 2$), K_{a1} (see above), and $pK_w = 13.8$ (refined through acid−base titration), we calculated the stability constants β_2 for the meta and para isomers (Table 2). The binding of imidazole to water-insoluble iron porphyrins, on the basis of the work of Pasternack et al.[44] and Walker et al,[40,41] is significantly stronger (up to several orders of magnitude) than the binding of 1-methylimidazole. We may expect higher β_2 values for imidazole than for 1-methylimidazole complexes of water-soluble iron porphyrins also. Accordingly, our β_2 for $Fe^{III}TM\text{-}4\text{-}PyP(1\text{-}MeIm)_2^{5+}$ is lower than β_2 reported by Pasternack et al.[44] for $Fe^{III}TM\text{-}4\text{-}PyP(Im)_2^{5+}$ (Table 2).[44] Our β_2 value for the meta isomer is lower than that for the para isomer, which might be explained by the greater steric restriction imposed by the meta porphyrin on an approaching imidazole.[13a,50,51]

Since the $Fe^{III}TM\text{-}2\text{-}PyP^{5+}$ (ortho isomer) is a mixture of atropoisomers, the spectral data did not exhibit clean isosbestic points (Figure 1). Figure 1C(2) shows the result when absorbance data at 586 nm were fitted to eq 6. The slope of 0.8 suggests binding of one imidazole throughout the experiment. Thus, the spectral data were explained in terms of a stepwise binding of imidazoles. From the first eight spectra (concentrated around the first approximate isosbestic point), we obtained $K_1 = \beta_1 = 1.2 \times 10^6$ M^{-1} related to eq 7 (Table 2, Figure 1).

The β_1 ($=K_1$) value represents an average value for the mixture of atropoisomers. The rest of the data (up to the "limiting" spectrum when no further increase in absorbance had been observed) correspond to the binding of a second imidazole, as described by eq 8.

By applying an appropriate form of eq 8, we obtained $K_2 = 16$ M^{-1}, which is much lower than K_1. According to our voltammetry data (see below), the di-ortho-substituted porphyrins show very weak binding of imidazole (as measured by insignificant changes in $E_{1/2}$ in the presence of imidazole). Thus we conclude that the first imidazole, in case of the ortho isomer, $Fe^{III}TM\text{-}2\text{-}PyP^{5+}$, binds to the open side of the metal center as previously proposed for the "picket-fence" porphyrins.[52]

Electrochemistry of Manganese Porphyrins. Our data, given in previous reports[13a,14] and in this study (Table 1), show that the metal-centered redox potential of Mn(III) porphyrins (Mn(III)/Mn(II)) is as sensitive to the presence of an axial ligand and to any substitution on the porphyrin ring as is the redox potential of analogous Fe(III) porphyrins. However, the manganese center shows a lower tendency toward axial ligation than the iron center,[36−39] as observed by cyclic voltammetry herein for water-soluble porphyrins and previously by Kelly and Kadish[53] and Bottomley and Kadish[54] for water-insoluble TPP types of porphyrins. Under moderate conditions, significant binding of the imidazole or hydroxo ligand does not occur, since the same redox potential for $Mn^{III}TM\text{-}2\text{-}PyP^{5+}$ was obtained at pH 2 and 7.8, and at pH 7.8 in the presence of 0.1 M 1-methylimidazole, as shown in Figure 2A. We ascribe these voltammograms to the aqua species $Mn^{III}TM\text{-}2\text{-}PyP(H_2O)^{5+}$. For comparison Figure 2B gives voltammograms of the aqua, hydroxo, and bis(imidazolato) forms of $Fe^{III}TM\text{-}2\text{-}PyP^{5+}$ under identical conditions of pH 2 and 7.8 in the absence and presence of 0.1 M 1-methylimidazole. It has been suggested by Harriman and Porter,[55] on the basis of spectral data, that at pH 8.5 the para isomer $Mn^{III}TM\text{-}4\text{-}PyP^{5+}$ has one OH^- and above pH 10.5 two OH^- ligands in axial positions ($pK_{a1} = 8.0$ and $pK_{a2} = 10.6$). For contrast, Balabura and Kirby[56] were able to spectrally detect only one protonation equilibrium of the para isomer with $pK_{a1} = 10.3$. We have detected no change in $E_{1/2}$ below pH 9 for any of the three isomers, ortho, meta, and para.[6,57] Harriman[58] did not detect any pH dependence of $E_{1/2}$ for the para isomer throughout the range pH 5−11. On the basis of the impact of the porphyrin substitution and metal center ligation on the electrochemical behavior observed throughout our study, it is highly likely that the replacement of axial water by OH^- would affect the redox potential. Our data[6,57] show that, at higher pH, i.e above pH 9 for the ortho isomer and above pH 10.5 for the meta and para isomers, $E_{1/2}$ shifts negatively. On the basis of the observed negative shift in $E_{1/2}$ by an average of 136 mV upon substitution of axial water by the hydroxo ligand in the case of isomers of $Fe^{III}TMPyP^{5+}$ (Table 1) and on the basis of our preliminary results on the pH dependence of $E_{1/2}$ for the

(49) *Handbook of Chemistry and Physics*, 74th ed.; Lide, D. R., Ed.; CRC: Boca Raton, FL, 1993−1994.
(50) Panicucci, R.; Bruice, T. C. *J. Am. Chem. Soc.* **1990**, *112*, 6063.
(51) Mizutani, T.; Horiguchi, T.; Koyama, H.; Uratani, I.; Ogoshi, H. *Bull. Chem. Soc. Jpn.* **1998**, *71*, 413.
(52) Collman, J. P.; Gagne, R. R.; Reed, C. A.; Halbert, T. R.; Lang, G.; Robinson, W. R. *J. Am. Chem. Soc.* **1975**, *97*, 1427.
(53) Kelly, S. L.; Kadish, K. M. *Inorg. Chem.* **1982**, *21*, 3631.
(54) Bottomley, L. A.; Kadish, K. M. *Inorg. Chem.* **1981**, *20*, 1348.
(55) Harriman, A.; Porter, G. *J. Chem. Soc., Faraday Trans. 2* **1979**, *75*, 1532.
(56) Balabura, R. J.; Kirby, R. A. *Inorg. Chem.* **1994**, *33*, 1021.
(57) Batinić-Haberle, I.; Spasojevic, I. Unpublished data.
(58) Harriman, A. *J. Chem. Soc., Dalton Trans.* **1984**, 141.

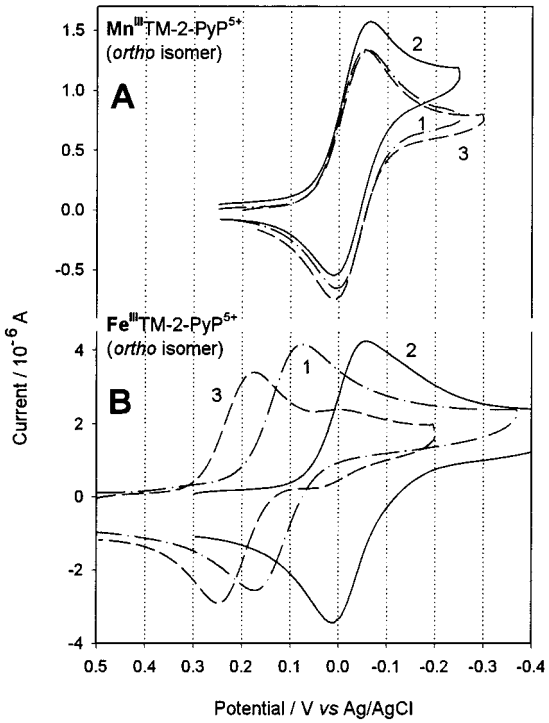

Figure 2. Cyclic voltammetry of 0.5 mM $Mn^{III}TM$-2-PyP^{5+} (A) and $Fe^{III}TM$-2-PyP^{5+} (B) at pH 2 (0.1 M NaCl) (1), at pH 7.8 (0.05 M phosphate buffer, 0.1 M NaCl) (2), and at pH 7.8 (0.05 M phosphate buffer, 0.1 M NaCl) in the presence of 0.1 M 1-methylimidazole (3). Potentials are in V vs Ag/AgCl and are shifted 255 mV negatively compared to the NHE.

meta and ortho isomers of the Mn porphyrin,[6,57] we estimate the pK_{a1} for the ortho, meta, and para isomers to be ~10.5, ~12.5, and ~12.5, respectively. These estimates are consistent with the pK_a of 11.4 reported for $Mn^{III}T(TMA)P^{5+}$.[59]

Reversible voltammograms were obtained in the case of cationic manganese porphyrins as well as in the case of $Mn^{III}TCPP^{3-}$ and $Mn^{III}TSPP^{3-}$, while quasi-reversible behavior was observed with other anionic porphyrins, notably with $Mn^{III}T(2,6\text{-}Cl_2\text{-}3\text{-}SO_3\text{-}P)P^{3-}$ and $Mn^{III}T(2,6\text{-}F_2\text{-}3\text{-}SO_3\text{-}P)P^{3-}$. The data are summarized in Table 1.

Electrochemistry of Iron Porphyrins. (a) pH 2. The reversible voltammograms of iron porphyrins obtained at pH 2 are ascribed to the high-spin iron(III) species[47] with an axial water molecule (Table 1).[19,20,48] The values obtained here, at pH 2 for $Fe^{III}TM$-2-$PyP(H_2O)^{5+}$ and $Fe^{III}TM$-4-$PyP(H_2O)^{5+}$, agree well with literature data.[19,20]

(b) Monomer/Dimer Equilibiria. At pH 7.8 and at 0.5 mM porphyrin, monomeric and dimeric species are in equilibrium. On the basis of the dimerization constants of iron porphyrins (eq 4), K_d of 2×10^3 M^{-1} for $Fe^{III}TM$-4-PyP^{5+} [48] and 8×10^5 M^{-1} for $Fe^{III}TSPP^{3-}$,[60] 61.8% and 4.8%, respectively, of the metalloporphyrins are monomeric at 0.5 mM. We may assume that K_d values are similar for the similar porphyrins $Fe^{III}TM$-3-PyP^{5+}, $Fe^{III}T(TMA)P^{5+}$, and $Fe^{III}TCPP^{3-}$, while sterically hindered molecules, i.e. ortho-substituted porphyrins, are not expected to dimerize to an observable degree.[50,36,61] Thus Su and co-workers[19] reported a significantly lower value, i.e. $K_d = 2 \times 10^2$ M^{-1} for $Fe^{III}TM$-2-PyP^{5+}, i.e. 91.6% of the porphyrin is monomeric at 0.5 mM. Indeed, we observed no voltammetric wave related to the dimer species in the voltammograms of $Fe^{III}TM$-2-PyP^{5+}, $Fe^{III}TE$-2-PyP^{5+}, $Fe^{III}T(2,6\text{-}Cl_2\text{-}3\text{-}SO_3\text{-}P)P^{3-}$ and $Fe^{III}T(2,4,6\text{-}Me_3\text{-}3,5\text{-}(SO_3)_2\text{-}P)P.^{7-}$ At a slow scan rate (10 mV/s) the reduction waves for both monomer and dimer were observed in the case of $Fe^{III}TM$-3-PyP^{5+} and $Fe^{III}TM$-4-PyP^{5+} in agreement with observations of Forshey and Kuwana.[20] Upon reduction of the iron to the divalent state, the dimer dissociates. Monomer/dimer equilibrium is slow, it takes 60−90 min for monomer/dimer equilibration at pH 8 at 0.1 mM $Fe^{III}TM$-4-PyP^{5+}.[20,48] Thus, when voltammograms were obtained at a scan rate of 100 mV/s only one reversible couple was observed, which was assigned to monomeric iron(III) species.

(c) Proton Dissociation Equilibrium. The axially ligated water of the cationic $Fe^{III}TM$-4-PyP^{5+}, $Fe^{III}TM$-3-PyP^{5+}, and $Fe^{III}TM$-2-PyP^{5+} has pK_{a1} = 5.5,[48] pK_{a1} = 5.9,[47] and pK_{a1} = 5.1,[19] while the that of anionic $Fe^{III}TSPP^{3-}$ and $Fe^{III}CPP^{3-}$ has pK_{a1} = 7.0[60] and pK_{a1} = 6.7,[62] and that of $Fe^{III}T(TFTMA)P^{5+}$ has pK_{a1} = 6.0.[63] Therefore, at pH 7.8, the predominant monomeric species of these iron porphyrins are in the high-spin[47] monohydroxo form. The pK_a values of the pyrrolic nitrogens and the metal-centered redox potentials are a measure of the effective positive charge at the metal center,[64] and thus a measure of the pK_a of the axially ligated water. On the basis of this reasoning, we assume that at pH 7.8 $Fe^{III}T(TMA)P^{5+}$ exists as a monohydroxo species as well. It has been reported that pK_{a1} = 6.55 for $Fe^{III}T(2,6\text{-}Me_2\text{-}3\text{-}SO_3\text{-}P)P^{3-}$.[65] With dominant electron donation through an inductive effect and direct overlap of the electron cloud of the ortho methyl group and π system of porphyrin ring,[66] we may expect that an additional methyl group at the para position would not affect pK_{a1} significantly; thus $Fe^{III}T(2,4,6\text{-}Me_3\text{-}3,5\text{-}(SO_3)_2\text{-}P)P^{7-}$ would exist as a monohydroxo species at pH 7.8. The cyclic voltammograms of monohydroxoiron(III) porphyrins are proton-dependent (eq 9), as observed here and elsewhere.[19,20] (The overall charges on porphyrin are omitted for simplicity.) At pH

$$Fe^{III}P(OH) + e^- + H^+ \rightleftharpoons Fe^{II}P(H_2O) \qquad (9)$$

7.8, the $E_{1/2}$ values of the iron(III) compounds that have an axial hydroxo ligand, instead of an axial water, are more negative by ≥100 mV (Table 1). The same has been previously observed in the case of apolar iron porphyrins[67] and the cationic porphyrins $Fe^{III}TM$-2-$PyP(OH)^{4+}$ and $Fe^{III}TM$-4-$PyP(OH)^{4+}$.[19] The reported proton dissociation constants for the first and second coordinated waters of $Fe^{III}T(2,6\text{-}Cl_2\text{-}3\text{-}SO_3\text{-}P)P^{3-}$ are pK_{a1} = 4.1 and pK_{a2} = 7.8.[65] If we account for the reported pK_{a1} and pK_{a2}, there would be equal amounts of monohydroxo and dihydroxo species of $Fe^{III}T(2,6\text{-}Cl_2\text{-}3\text{-}SO_3\text{-}P)P^{3-}$ in solution at pH 7.8. However, when the $E_{1/2}$ values and the proton dissociation constants of the pyrrolic nitrogens of $Fe^{III}T(2,6\text{-}Cl_2\text{-}3\text{-}SO_3\text{-}P)P^{3-}$ and $Fe^{III}TM$-2-PyP^{5+} are compared, one would expect an equal or a higher pK_a for the axial water of the former than of the latter compound. Consequently, both porphyrins should be in their monohydroxo forms at pH 7.8.

(59) Bettelheim, A.; Ozer, D.; Parash, R. *J. Chem. Soc., Faraday Trans. 1* **1983**, *79*, 1555.
(60) El-Awady, A. A.; Wilkins, P. C.; Wilkins, R. G. *Inorg. Chem.* **1985**, *24*, 2053.
(61) Murata, K.; Panicucci, R.; Gopinath, E.; Bruice, T. C. *J. Am. Chem. Soc.* **1990**, *112*, 6072.
(62) (a) Miskelly, G. M.; Webley, W. S.; Clark, C. R.; Buckingham. D. A. *Inorg. Chem.* **1988**, *27*, 3773. (b) Stong, J. D.; Hartzell, C. R. *Bioinorg. Chem.* **1976**, *5*, 219.
(63) La, T.; Richards, R.; Miskelly, G. M. *Inorg. Chem.* **1994**, *33*, 3159.
(64) Boucher, L. J.; Garber, H. K. *Inorg. Chem.* **1970**, *9*, 2644.
(65) Jeon, S.; Bruice, T. C. *Inorg. Chem.* **1992**, *31*, 4843.
(66) Koerner, R.; Wright, J. L.; Ding, X. D.; Nesset, M. J. M.; Aubrecht, K.; Watson, R. A.; Barber, R. A.; Mink, L. M.; Tipton, A. R.; Norvell, C. J.; Skidmore, K.; Simonis, U.; Walker, F. A. *Inorg. Chem.* **1998**, *37*, 733.
(67) Lexa, D.; Momenteau, M.; Saveant, J.-M.; Xu, F. *Inorg. Chem.* **1985**, *24*, 122.

At pH 7.8, voltammograms of the cationic Fe porphyrins are reversible. The voltammograms of negatively charged porphyrins are either quasi-reversible ($Fe^{III}T(2,6\text{-}Cl_2\text{-}3\text{-}SO_3\text{-}P)P^{3-}$, $Fe^{III}T(2,4,6\text{-}Me_3\text{-}3,5\text{-}(SO_3)_2\text{-}P)P^{7-}$) or irreversible ($Fe^{III}TCPP^{3-}$, $Fe^{III}TSPP^{3-}$).

(d) pH 7.8 with 1-Methylimidazole. On the basis of the stability constants given in Table 2, $Fe^{III}TM\text{-}3\text{-}PyP(1\text{-}MeIm)_2^{5+}$ and $Fe^{III}TM\text{-}4\text{-}PyP(1\text{-}MeIm)_2^{5+}$ exist in aqueous 0.1 M 1-methylimidazole solution at pH 7.8. On the basis of similar β_2 values given in the literature for the TMPyP and TSPP series[44] and for a variety of other iron porphyrins,[40,41] we may also assume that, at 0.1 M imidazole, $Fe^{III}TSPP(1\text{-}MeIm)_2^{3-}$ and $Fe^{III}TCPP(1\text{-}MeIm)_2^{3-}$ are the major species in solution, as is $Fe^{III}T(TMA)P(1\text{-}MeIm)_2^{5+}$. Reversible voltammograms were obtained for the imidazole complexes of all of the Fe porphyrins mentioned above. The $E_{1/2}$ values, in volts vs NHE, are given in Table 1. The shift in $E_{1/2}$ between the high-spin state with an axially ligated water and the species with two axially coordinated imidazoles, found in the case of both ortho compounds, $Fe^{III}TM\text{-}2\text{-}PyP^{5+}$ and $Fe^{III}TE\text{-}2\text{-}PyP^{5+}$ (Table 1), equals the shift observed in the case of para and meta $Fe^{III}TMPyP^{5+}$ and $Fe^{III}TSPP^{3-}$, where evidence for bis(imidazole) complexes has been found here and elsewhere.[44-46] The change from high-spin to low-spin states has been thought to promote bis(imidazole) complex formation.[41,47,68] Our CV data, in addition to β_2 values, suggest that $Fe^{III}TM\text{-}2\text{-}PyP^{5+}$ and $Fe^{III}TE\text{-}2\text{-}PyP^{5+}$ form bis(imidazole) complexes under our experimental conditions. Yet some ambiguity[52,66] still exists in the literature for whether mono(imidazole) or bis(imidazole) species dominate in the case of sterically hindered ortho type porphyrins. Iron bis(imidazole) complexes are ~220 mV more easily reduced than monohydroxoiron porphyrins (Table 1). The voltammograms of $Fe^{III}TM\text{-}2\text{-}PyP(H_2O)^{5+}$ at pH 2, $Fe^{III}TM\text{-}2\text{-}PyP(OH)^{4+}$ at pH 7.8, and $Fe^{III}TM\text{-}2\text{-}PyP(1\text{-}MeIm)_2^{5+}$ at pH 7.8 are shown in Figure 2. Porphyrins that are substituted at both ortho positions, i.e. $Fe^{III}T(2,6\text{-}Cl_2\text{-}3\text{-}SO_3\text{-}P)P^{3-}$, $Fe^{III}T(2,4,6\text{-}Me_3\text{-}3,5\text{-}(SO_3)_2\text{-}P)^{7-}$, and $Fe^{III}T(TFTMA)P^{5+}$, showed negligible imidazole-dependent shifts in redox potential, presumably due to the restricted access of imidazole to the metal center.

SOD Activity in Vitro. Only those porphyrins were investigated whose metal-centered redox potentials were sufficiently positive to allow significant SOD-like activity. The SOD activities, calculated from the competition kinetics,[13a] are given in Table 3 as IC_{50} and log k_{cat}. IC_{50} represents the porphyrin concentration that causes 50% inhibition of cytochrome *c* reduction by $O_2^{\bullet-}$.[13a] The rate of cytochrome *c* reduction by $O_2^{\bullet-}$, $k_{cyt} = 2.6 \times 10^5\ M^{-1}\ s^{-1}$,[32,33] was used to calculate log k_{cat}. Ionic strength was varied from 0.01 to 0.5 M in order to verify that porphyrin, like the SOD enzyme,[69-71] reacts with deprotonated $O_2^{\bullet-}$ rather than with $HO_2^{\bullet}$. The inhibition of cytochrome *c* reduction by $Mn^{III}TE\text{-}2\text{-}PyP^{5+}$ was decreased by increasing ionic strength, as expected when the reactive species are of opposite charge. As discussed above, the data in Table 3 correspond to aquamanganese porphyrins and monohydroxoiron species. The exceptions are $Fe^{III}TCPP^{3-}$ and $Fe^{III}TSPP^{3-}$. On the basis of its K_d value of $8 \times 10^5\ M^{-1}$, $Fe^{III}TSPP^{3-}$ is 73.5% in its dimeric form[47] at $IC_{50} = 1.3 \times 10^{-5}$ M. The same should be true for the similar anionic porphyrin $Fe^{III}TCPP^{3-}$ at similar IC_{50} of 2.1×10^{-5} M. The catalytic rate constant obtained here, by cytochrome *c* SOD assay, for the para isomer $Fe^{III}TM\text{-}4\text{-}PyP(OH)^{4+}$, $k_{cat} = 1.6 \times 10^7\ M^{-1}\ s^{-1}$, is similar to the value obtained by the stopped-flow technique by Groves and coworkers,[16] $k_{cat} = 1.9 \times 10^7\ M^{-1}\ s^{-1}$, as well as to other results obtained by indirect assay.[72,73] The same is true for the aquamanganese analogue.[13a,16] In no case was SOD-like activity of the metal-free porphyrins detected. No significant SOD-like activity of $Fe^{III}TM\text{-}2\text{-}PyP(1\text{-}MeIm)_2$ and $Fe^{III}TM\text{-}4\text{-}PyP(1\text{-}MeIm)_2$ has been observed despite the 220 mV more positive $E_{1/2}$ of the bis(imidazole) complexes than of their monohydroxo analogues (Table 1). This is consistent with the 2 order of magnitude lower rate constant reported for the reduction of $Fe^{III}TM\text{-}4\text{-}PyP(1\text{-}MeIm)_2^{5+}$ by $O_2^{\bullet-}$ (0.1 M formic acid, $k_{red} = 1.1 \times 10^6\ M^{-1}\ s^{-1}$) when compared to the reduction of the aqua complex of $Fe^{III}TM\text{-}4\text{-}PyP^{5+}$ by $O_2^{\bullet-}$ (0.3 M formic acid, $k_{red} = 3.1 \times 10^8\ M^{-1}\ s^{-1}$).[74,75] The different mechanisms offered for the aqua and bis(imidazole) complexes are consistent with our observation (see Discussion—$E_{1/2}$ vs log k_{cat} dependence).[74,75] As expected, due to the lower tendencies of manganese porphyrins toward axial ligation, the SOD-like activity of $Mn^{III}TMP\text{-}2\text{-}PyP^{5+}$ was not affected by methylimidazole. Due to the slow dimer/monomer equilibria of iron porphyrins, 1 mM iron porphyrins in aqueous/acidic (pH 2) stock solutions were used to favor the monomer.

Table 3. SOD-like Activity of Monohydroxoiron(III) and Aquamanganese(III) Porphyrins Determined in 0.05 M Phosphate Buffer, pH 7.8, at 25 °C

metalloporhyrin	log $k_{cat}(O_2^{\bullet-})$[a]	IC_{50}, M[b]
$M^{III}TE\text{-}2\text{-}PyP^{5+}$ (**1_{Mn}**)	7.76	4.5×10^{-8}
$Mn^{III}TM\text{-}2\text{-}PyP^{5+}$(**$2_{Mn}$**)	7.79	4.3×10^{-8}
$Mn^{III}BM\text{-}2\text{-}PyP^{3+}$ (**$2a_{Mn}$**)	6.52	7.8×10^{-7}
$Mn^{III}TrM\text{-}2\text{-}PyP^{4+}$(**$2b_{Mn}$**)	6.63	6.1×10^{-7}
$Mn^{III}TM\text{-}3\text{-}PyP^{5+}$ (**3_{Mn}**)	6.61	6.4×10^{-7}
$Mn^{III}TM\text{-}4\text{-}PyP^{5+}$ (**4_{Mn}**)	6.58	6.8×10^{-7}
$Mn^{III}T(TMA)P^{5+}$ (**5_{Mn}**)	5.11	2.0×10^{-5}
$Mn^{III}T(TFTMA)P^{5+}$ (**8_{Mn}**)	6.02	2.5×10^{-6}
$Mn^{III}TCPP^{3-}$ (**9_{Mn}**)	4.56	7.2×10^{-5}
$Mn^{III}T(2,6\text{-}Cl_2\text{-}3\text{-}SO_3\text{-}P)P^{3-}$ (**11_{Mn}**)	6.00	2.6×10^{-6}
$Mn^{III}T(2,6\text{-}F_2\text{-}3\text{-}SO_3\text{-}P)P^{3-}$ (**13_{Mn}**)	5.51	8.0×10^{-6}
$Fe^{III}TE\text{-}2\text{-}PyP(OH)^{4+}$ (**1_{Fe}**)	8.00	2.6×10^{-8}
$Fe^{III}M\text{-}2\text{-}PyP(OH)^{4+}$ (**2_{Fe}**)	7.95	2.9×10^{-8}
$Fe^{III}TM\text{-}3\text{-}PyP(OH)^{4+}$ (**3_{Fe}**)	7.42	9.8×10^{-8}
$Fe^{III}TM\text{-}4\text{-}PyP(OH)^{4+}$ (**4_{Fe}**)	7.20	1.6×10^{-7}
$Fe^{III}T(TMA)P(OH)^{4+}$ (**5_{Fe}**)	6.07	2.2×10^{-6}
$Fe^{III}TSPP(OH)^{4-}$[c] (**10_{Fe}**)	5.10	2.1×10^{-5}
$Fe^{III}TCPP(OH)^{4-}$[c] (**9_{Fe}**)	5.30	1.3×10^{-5}

[a] k_{cat} in $M^{-1}\ s^{-1}$; errors are ±10%. [b] IC_{50} of Cu,Zn−SOD is 1.3×10^{-9} M.[32,33] IC_{50} is the concentration of the porphyrin that causes 50% of the inhibition of cytochrome *c* reduction by $O_2^{\bullet-}$. No significant SOD-like activity of $Mn^{III}T(\alpha,\alpha,\alpha,\alpha\text{-}2\text{-}MINP)^{5+}$ has been observed. [c] Based on $K_d = 8 \times 10^5\ M^{-1}$ for $Fe^{III}TSPP^{3-}$,[60] 73.5% of it is present as a dimer at its IC_{50} concentration, as should be the case for the anionic $Fe^{III}TCPP^{3-}$.

Oxidative Degradation of Porphyrins with H_2O_2. The reactions between H_2O_2 and the porphyrins were followed at pH 7.8 where H_2O_2 ($pK_a = 11.6$),[76] aquamanganese and monohydroxoiron porphyrins were major species in solution. In the presence of excess hydrogen peroxide second-order rate constants were determined from linear plots of the observed pseudo-first-order rate constants vs $[H_2O_2]$, $k_{obs} = k[H_2O_2]$, and

(68) Owen, J.; Harris, E. A. In *Electron Paramagnetic Resonance*; Geschwind, S., Ed.; Plenum Press: New York, 1972.
(69) Klug, D.; Rabani, J.; Fridovich, I. *J. Biol. Chem.* **1972**, *247*, 4839.
(70) Cudd, A.; Fridovich, I. *J. Biol. Chem.* **1982**, *257*, 11443.
(71) Cudd, A.; Fridovich, I. *FEBS Lett.* **1982**, *144*, 181.
(72) Pasternack, R. F.; Halliwell, B. *J. Am. Chem. Soc.* **1979**, *101*, 1026.
(73) Pasternack, R. F.; Skowronek, W. R., Jr. *J. Inorg. Biochem.* **1979**, *11*, 261.
(74) Soloman, D.; Peretz, P.; Faraggi, M. *J. Phys. Chem.* **1982**, *86*, 1842.
(75) Faraggi, M.; Peretz, P.; Weinraub, D. *Int. J. Radiat. Biol.* **1986**, *49*, 951.
(76) Everett, A. J.; Minkoff, G. J. *Trans. Faraday Soc.* **1953**, *49*, 410.

Table 4. Second-Order Rate Constants for the Oxidative Degradation of *N*-Alkylpyridiniumyl Porphyrins by Hydrogen Peroxide at 25 °C[a]

porphyrin	$k(H_2O_2)$, M^{-1} s^{-1}
$H_2TM\text{-}2\text{-}PyP^{4+}$ (**2**)	5×10^{-6}
$ZnTM\text{-}2\text{-}PyP^{4+}$ ($\mathbf{2_{Zn}}$)	5×10^{-6}
$Mn^{III}TE\text{-}2\text{-}PyP^{5+}$ ($\mathbf{1_{Mn}}$)	1.3
$Mn^{III}TM\text{-}2\text{-}PyP^{5+}$ ($\mathbf{2_{Mn}}$)	1.3
$Mn^{III}TM\text{-}3\text{-}PyP^{5+}$ ($\mathbf{3_{Mn}}$)	4.9
$Mn^{III}TM\text{-}4\text{-}PyP^{5+}$ ($\mathbf{4_{Mn}}$)	4.6
$Fe^{III}TM\text{-}2\text{-}PyP(OH)^{4+}$ ($\mathbf{2_{Fe}}$)	23
$Fe^{III}TM\text{-}3\text{-}PyP(OH)^{4+}$ ($\mathbf{3_{Fe}}$)	38

[a] Conditions: 6 μM porphyrin, 50 μM−0.5 M hydrogen peroxide, pH 7.8, 0.1 M NaCl, 0.05 M phosphate buffer; errors are ±10%.

are listed in Table 4. It has been established[36,39,42,50,65,77] that the reactions of metalloporphyrins with hydroperoxides are first order in both H_2O_2 and porphyrin, consistent with our observations. The reactions were proposed to proceed through high-valent manganese and iron species with O−O scission as the rate-determining step. The transient high-valent metalloporphyrin intermediates are further capable of oxidative destruction of the porphyrin ring as shown in Figure 3. By spectrophotometric rapid-scanning of the reaction between $Mn^{III}TM\text{-}2\text{-}PyP^{5+}$ and H_2O_2 (Figure 3A), we recorded the destruction of the manganese porphyrin, but also the appearance of the transient high-valent manganese species with $\lambda_{max} \sim 430$ nm.[55,78] On the basis of the available spectral data ($\lambda = 422$ nm)[55,58,78b] for O=$Mn^{IV}TM\text{-}4\text{-}PyP^{4+}$, we ascribe the peak at 430 nm to the Mn(IV) porphyrin. In the case of $Fe^{III}TM\text{-}2\text{-}PyP(OH)^{4+}$, only the first few scans occurred with an isosbestic point between 500 and 650 nm, indicating the accumulation of another species, presumably high-valent iron porphyrin (Figure 3B). This was followed by bleaching of the porphyrin, suggesting a much faster disappearance of transient high-valent iron species than in the case of Mn porphyrin (Figure 3B). No effect of mannitol on the rate constant of either $Fe^{III}TM\text{-}2\text{-}PyP(OH)^{4+}$ or $Mn^{III}TM\text{-}2\text{-}PyP^{5+}$ was observed, thus eliminating a role for $OH^{\bullet}$ radicals in the oxidation of the porphyrin ring. The labilizing trans effect[36,39,50,79] of the OH^- ligand has been observed, whereby hydroxoiron porphyrins react much faster than the corresponding aqua compounds. We[6] and others[19,37,58,78] have found that the redox potentials for one-electron metal-centered oxidations (M(IV)/M(III)) are very similar for different porphyrins (TMPyP,[6,19] TSPP,[58,78] TCPP[58,78] series) and different metal centers (Fe and Mn),[6,19,37] Therefore, it is likely that the more than 1 order of magnitude decrease in stability of the Fe porphyrins relative to the Mn compounds (Table 4) is the consequence of the effect of the OH^- ligand of monohydroxoiron(III) porphyrins, rather than of their redox potentials.[39] Applying the same reasoning, we have observed no ortho effect on the reactivity toward H_2O_2 of a magnitude comparable to the ortho effect upon the dismutation of $O_2^{\bullet -}$.[13a]

Complementation of the *sodAsodB E. coli.* It has been[13a] shown that, at 25 μM, all isomers of $Mn^{III}TMPyP^{5+}$ afforded protection for *sodAsodB E. coli* grown in a casamino acid medium, but only the ortho and meta isomers did so when *E. coli* was grown in a minimal medium. Therefore only the ortho isomers, $Mn^{III}TM\text{-}2\text{-}PyP^{5+}$ and $Mn^{III}TE\text{-}2\text{-}PyP^{5+}$, were again tested. All the isomers of $Fe^{III}TMPyP^{5+}$ and $Fe^{III}TE\text{-}2\text{-}PyP^{5+}$ were investigated, as well as $Fe^{III}T(TMA)P^{5+}$, $Fe^{III}TCPP^{3-}$, $Fe^{III}T(TFTMA)P^{5+}$, $Fe^{III}TSPP^{3-}$, $Mn^{III}T(2,6\text{-}Cl_2\text{-}3\text{-}SO_3\text{-}P)P^{3-}$, $Mn^{III}T(2,6\text{-}F_2\text{-}3\text{-}SO_3\text{-}P)P^{3-}$, $Mn^{III}T(TFTMA)P^{5+}$, $Mn^{III}T(2,4,6\text{-}Me_3\text{-}3,5\text{-}(SO_3)_2\text{-}P)P^{7-}$, $Mn^{III}(\alpha,\alpha,\alpha,\alpha\text{-}2\text{-}MINP)P^{5+}$, $Mn^{III}T(TMA)P^{5+}$, and $Mn^{III}TCPP^{3-}$. The effects of these compounds on *E. coli* were studied under aerobic and anaerobic conditions and in both minimal and casamino acid media. Under all conditions, iron porphyrins were toxic to both SOD-deficient and SOD-proficient *E. coli.* Among Mn porphyrins, only $Mn^{III}TM\text{-}2\text{-}PyP^{5+}$ and $Mn^{III}TE\text{-}2\text{-}PyP^{5}$ are beneficial and afforded complete or partial protection. The bulkier ethylated analogue, $Mn^{III}TE\text{-}2\text{-}PyP^{5+}$, was slightly more beneficial than $Mn^{III}TM\text{-}2\text{-}PyP^{5+}$, as expected due to its lower degree of interaction with nucleic acids.[13a,80] These data are given in Figures 4−6.

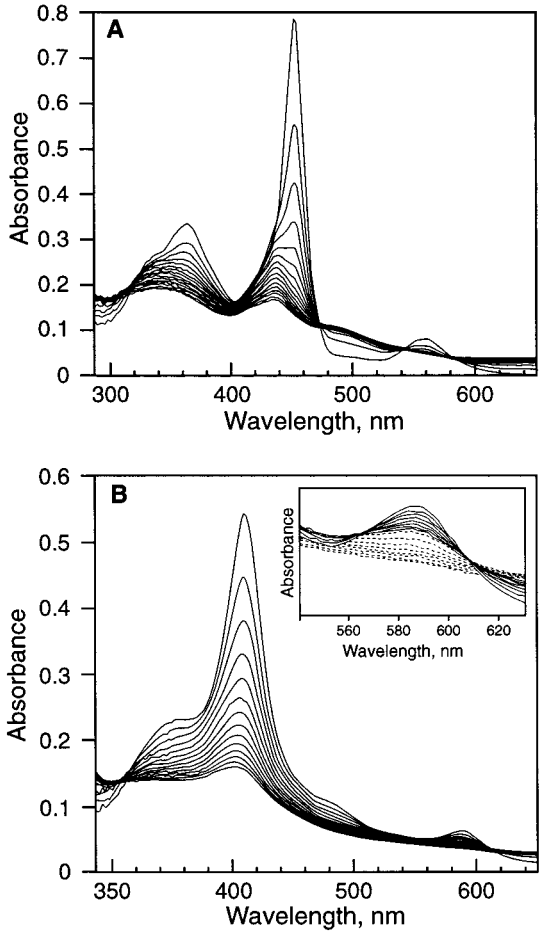

Figure 3. Rapid scans of the reaction of $Mn^{III}TM\text{-}2\text{-}PyP^{5+}$ (A) and $Fe^{III}TM\text{-}2\text{-}PyP(OH)^{4+}$ (B) with H_2O_2 at pH 7.8 (0.05 M phosphate buffer), 6 μM porphyrin concentration, and 5 mM (A) and 0.2 mM H_2O_2 (B) concentration at 25 °C. Scans were taken in 32 s intervals from 0.64 to 516 s (A) and in 39 s intervals from 2.6 to 516 s (B).

Discussion

SOD-like activities, expressed in terms of the catalytic rate constants for the dismutation of $O_2^{\bullet -}$, were determined at pH 7.8, where the iron porphyrins bear an axial hydroxo ligand and the manganese porphyrins are in the aqua form. The data are presented in Table 3. The catalytic cycle includes the reduction of Mn(III) porphyrin by one molecule of $O_2^{\bullet -}$

(77) Murata, K.; Panicucci, R.; Gopinath, E.; Bruice, T. C. *J. Am. Chem. Soc.* **1990**, *112*, 6072.
(78) (a) Carnieri, N.; Harriman, A.; Porter, G. *J. Chem. Soc., Dalton Trans.* **1982**, 931. (b) Liu, M.-H.; Su, Y. O. *J. Electroanal. Chem. Interfacial Electrochem.* **1997**, *426*, 197. (c) Harriman, A.; Porter, G. *J. Chem. Soc., Faraday Trans. 2* **1979**, 1543.
(79) Mansuy, D.; Battioni, P.; Renaud, J.-P. *J. Chem. Soc., Chem. Commun.* **1984**, 1255.
(80) Batinić-Haberle, I.; Kachadourian, R. Unpublished results.

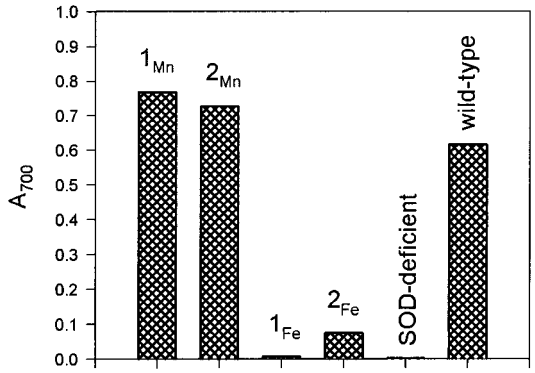

Figure 4. Growth of SOD-deficient *E. coli* JI132 after 56 h in a minimal (five amino acids) medium as affected by the presence of 25 μM concentrations of Mn^{III}TE-2-PyP^{5+}(**1$_{Mn}$**), Mn^{III}TM-2-PyP^{5+}(**2$_{Mn}$**), Fe^{III}TE-2-PyP^{5+}(**1$_{Fe}$**), and Fe^{III}TM-2-PyP^{5+}(**2$_{Fe}$**). Also shown is the growth of the SOD-deficient and SOD-proficient *E. coli* in the absence of porphyrin.

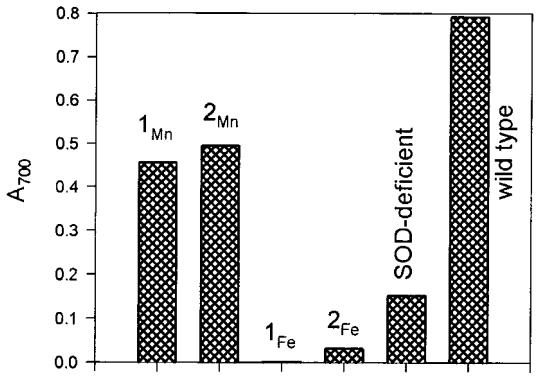

Figure 5. Growth of SOD-deficient *E. coli* JI132 after 4 h in a casamino acid medium as affected by the presence of 25 μM concentrations of Mn^{III}TE-2-PyP^{5+}(**1$_{Mn}$**), Mn^{III}TM-2-PyP^{5+}(**2$_{Mn}$**), Fe^{III}TE-2-PyP^{5+}(**1$_{Fe}$**), and Fe^{III}TM-2-PyP^{5+}(**2$_{Fe}$**). Also shown is the growth of SOD-deficient and SOD-proficient *E. coli* in the absence of porphyrin.

followed by the reoxidation of the same metalloporphyrin by

$$O_2^{\bullet -} + Mn^{III}P \rightarrow O_2 + Mn^{II}P^- \qquad k_{red} \qquad (10)$$

$$O_2^{\bullet -} + Mn^{II}P^- + 2H^+ \rightarrow H_2O_2 + Mn^{III}P \qquad k_{ox} \qquad (11)$$

another $O_2^{\bullet -}$ as shown in eqs 10−14.[81] (The notation of the overall porphyrin charges is simplified, whereby the porphyrin having metal in its +3 state is assigned as a neutral species.) In the case of monohydroxoiron(III) porphyrins, the porphyrin reduction step given by eq 12 is followed by the protonation of

$$O_2^{\bullet -} + Fe^{III}P(OH) \rightarrow O_2 + Fe^{II}P(OH)^- \qquad k_{red} \qquad (12)$$

$$Fe^{II}P(OH)^- + H^+ \rightleftharpoons Fe^{II}P(H_2O) \qquad K_{a1}^{-1} \qquad (13)$$

$$O_2^{\bullet -} + Fe^{II}P(H_2O) + H^+ \rightarrow H_2O_2 + Fe^{III}P(OH) \qquad k_{ox} \qquad (14)$$

the monohydroxoiron(II) porphyrin (eq 13), since the pK_{a1} values of the iron(II) porphyrins are several orders of magnitude higher than those of the corresponding iron(III) porphyrins.[47b,48] The reduction of Fe^{III}TM-4-PyP(OH)$^{4+}$ and Mn^{III}TM-4-PyP^{5+} (eqs 10 and 12) has been found to be 2−3 orders of magnitude

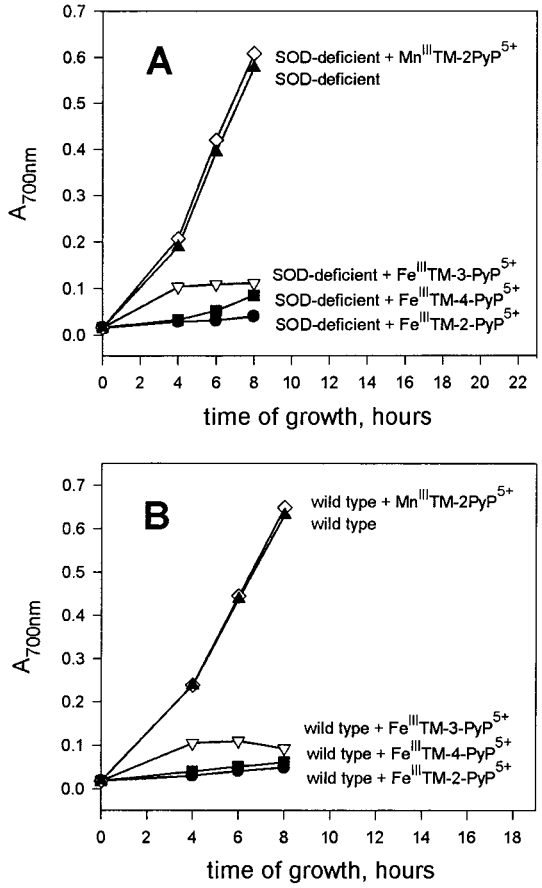

Figure 6. Growth curves of SOD-deficient *E. coli* JI132 (A) and wild-type AB1157 (B) in a casamino acid medium under anaerobic conditions as affected by the presence of 25 μM concentrations of ortho Mn^{III}TM-2-PyP^{5+} (diamonds), ortho Fe^{III}TM-2-PyP^{5+} (circles), meta Fe^{III}TM-3-PyP^{5+} (inverted triangles), and para Fe^{III}TM-4-PyP^{5+} (squares). The growth of JI132 in the absence of porphyrin (upright triangles) (A) as well as the growth of wild-type AB1157 (upright triangles) (B) was followed.

slower than their reoxidation; thus it is the rate-limiting step of the catalytic cycle.[5,16,72,82] (The same should hold for all the metalloporphyrins that are reduced with greater difficulty, i.e. of more negative $E_{1/2}$.) The pseudo-first-order rate constants for the catalysis of $O_2^{\bullet -}$ dismutation[5,16,72,75] by those and other water-soluble iron(III) and manganese(III) porphyrins thus relate to the rate-limiting reduction step. Plots of the pseudo-first-order rate constants vs porphyrin concentration were linear, showing that the fast protonation step in the case of iron(III) porphyrins does not affect the overall rate; i.e., the forward and reverse reactions are effectively second order.[5,16,45,72,75,83,84] Consequently, k_{cat} in Table 3 corresponds to the electron-transfer reaction described by eqs 10 and 12.

Figure 7 illustrates a plot of log k_{cat} as a function of $E_{1/2}$ for the Fe monohydroxo and Mn aqua porphyrins. The slope of the linear regression lines predicts a 10-fold increase in k_{cat} for a 120 mV increase in $E_{1/2}$. The rate of the catalytic cycle will still be limited by the reduction step even for those porphyrins having as much as 120 mV more positive redox potential than Fe^{III}TM-4-PyP(OH)$^{4+}$ and Mn^{III}TM-4-PyP^{5+}. The equivalent

(81) (a) Fridovich, I. *Annu. Rev. Biochem.* **1995**, *64*, 97. (b) Fridovich, I. *J. Exp. Biol.* **1998**, *201*, 1203.

(82) Faraggi, M. In $O_2^{\bullet -}$ *dismutation catalyzed by water soluble porphyrins. A pulse radiolysis study*; Bors, W., Saran, M., Tait, D., Eds.; Walter de Gruyter: Berlin, 1984; pp 419−430.

(83) McLaughlin, V. B.; Faraggi, M.; Leussing, D. L. *Inorg. Chem.* **1993**, *32*, 941.

(84) Peretz, P.; Solomon, D.; Weinraub, D.; Faraggi, M. *Int. J. Radiat. Biol.* **1982**, *42*, 449.

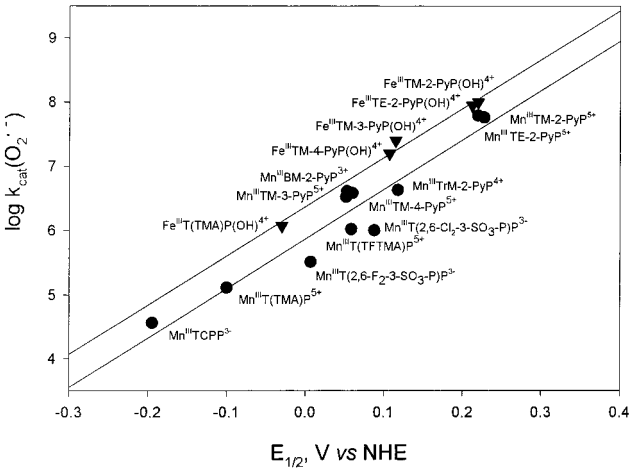

Figure 7. Reactivity of monohydroxoiron and aquamanganese porphyrins as catalysts for $O_2^{\bullet -}$ dismutation, expressed in terms of log $k_{cat}(O_2^{\bullet -})$ (Table 3), plotted as a function of the metal-centered redox potential, $E_{1/2}$ (Table 1). Waters are omitted for clarity. The slopes of the lines are 7.72 and 7.65 and the intercepts are 6.37 and 5.87 for Fe and Mn porphyrins, respectively.

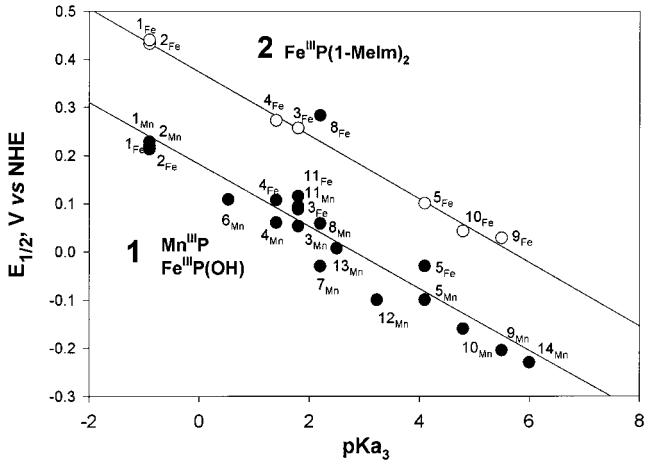

Figure 8. Metal-centered redox potentials for the M(III)/M(II) couples of iron and manganese porphyrins, $E_{1/2}$ vs pK_{a3}. The potentials of line 1 were obtained in aqueous solution, pH 7.8, 0.1 M NaCl, 0.05 M phosphate buffer and correspond to the monohydroxoiron porphyrins, $Fe^{III}P(OH)$, and aquamanganese(III) porphyrins, $Mn^{III}P$. Although reported[65] pK_a values of the axially ligated waters of $Fe^{III}T(2,6\text{-}Cl_2\text{-}3\text{-}SO_3\text{-}P)P^{3-}$ (**11_{Fe}**) point to 1:1 equilibria of $Fe^{III}P(OH)$ and $Fe^{III}P(OH)_2$, our plot suggests that $Fe^{II}P(OH)$ is the major species at pH 7.8 (see also Electrochemistry of Iron Porphyrins). The potentials of line 2 correspond to the bis(imidazolato) complexes, $Fe^{III}P(1\text{-}MeIm)_2$.

slopes for the Fe (7.72) and Mn (7.65) systems are consistent with those predicted by the simplified Marcus equation[85] (eq 15) for outer-sphere electron transfer, where k_{12} is k_{cat} and k_{11}

$$\log k_{12} = 0.5E_{1/2}/0.059 + 0.5 \log(k_{11}k_{22}) \qquad (15)$$

and k_{22} are the self-exchange rate constants for the metalloporphyrins and for $O_2^{\bullet -}$. From the Marcus equation and from the differences in intercepts, we calculate the ratio of self-exchange rate constants $k_{11}(FeP(OH))/k_{11}(MnP)$ to be ~8. This is consistent with the higher self-exchange rate constants for Fe over Mn porphyrins previously reported.[86,87] Due to the wide range of self-exchange rate constants reported for $O_2^{\bullet -}/O_2$ (from 10^{-8} to 3 M^{-1} s^{-1}),[85d,88] we have not attempted to calculate the absolute values of the self-exchange rate constants for the metalloporphyrins.

The metal-centered redox potentials, which are linearly related to log k_{cat}, are also linearly related to pK_{a3} for the acidic pyrrolic nitrogens, as shown in Figure 8. Empirical linear free energy relationships[89,90] between either metal-centered redox potential or porphyrin-centered reduction potential[91] and pK_a have been found previously for a variety of water-soluble and to a lesser degree for water-insoluble porphyrins.[92−98] The influence of the porphyrin structure on the acid dissociation constants of pyrrolic nitrogens, and on the metal-centered redox potentials was seen in all manganese and iron anionic and cationic porphyrins, as shown by lines 1 and 2 of the plot in Figure 8. At any given porphyrin pK_{a3}, the iron−imidazole complexes are 220 mV more easily reduced than their monohydroxo analogues. Yet this has not resulted in higher k_{cat} of bis(imidazole)iron porphyrins. Consequently the $E_{1/2}$ vs log k_{cat} dependence, given in Figure 7, is not applicable to this type of axially ligated iron porphyrin. A change in mechanism may be suspected.[74,75] A dramatic deviation from the plot in Figure 8 was obtained only in the case of $Fe^{III}T(TFTMA)P^{5+}$, whose high pK_{a3} can be rationalized, as can that of 2,6-disubstituted porphyrins,[27] on the basis of resonance and bending. From the interdependence of log k_{cat}, $E_{1/2}$, and pK_{a3}, we propose $E_{1/2}$ and/or pK_{a3} to be useful predictors of SOD-like activity.

Since H_2O_2 is a product of $O_2^{\bullet -}$ dismutation (eqs 11 and 14), the stability of metalloporphyrins toward H_2O_2 is relevant. We have shown that metalloporphyrins are more prone to oxidative degradation by H_2O_2 than their nonmetalated analogues, notably so in the case of iron porphyrins (Table 4). The process is affected by the redox capability of the metal center; e.g., no significant degradation occurs with $ZnTM\text{-}2\text{-}PyP^{4+}$, whose metal center is redox inactive (Table 4). It has previously been reported that porphyrins of more positive metal-centered (M(III)/M(II)) reduction potentials exhibit positively shifted porphyrin-centered reduction potentials.[99−105] Porphyrin-centered and metal-centered

(85) (a) Bennett, L. E. *Prog. Inorg. Chem.* **1973**, *18*, 1. (b) Marcus, R. A. *Annu. Rev. Phys. Chem.* **1964**, *15*, 155. (c) Marcus, R. A. *J. Chem. Phys.* **1965**, *43*, 679. (d) Jordan, R. B. *Reaction Mechanisms of Inorganic and Organometallic Systems*, 2nd ed.; Oxford University Press: New York, 1998.
(86) (a) Langley, R.; Hambright, P. *Inorg. Chem.* **1985**, *24*, 1267. (b) Langley, R.; Hambright, P.; Williams, R. F. X. *Inorg. Chim. Acta* **1985**, *104*, L25.
(87) Pasternack, R. F.; Spiro, E. G. *J. Am. Chem. Soc.* **1978**, *100*, 968.
(88) (a) Zahir, K.; Espenson, J. H.; Bakac, A. *J. Am. Chem. Soc.* **1988**, *110*, 5059. (b) Stanbury, D. M.; Haas, O.; Taube, H. *Inorg. Chem.* **1980**, *19*, 518.
(89) Hammet, C. P. *Physical Organic Chemistry*; McGraw-Hill: New York, 1940; p 184.
(90) Zuman, P. *Collect. Czech. Chem. Commun.* **1960**, *25*, 3265.
(91) Williams, R. F. X.; Hambright, P. *Bioinorg. Chem.* **1978**, *9*, 537.
(92) Worthington, P.; Hambright, P.; Williams, R. F. X.; Reid, J.; Burnham. C.; Shamim, A.; Turay, J.; Bell, D. M.; Kirkland, R.; Little, R. G.; Datta-Gupta, N.; Eisner, U. *J. Inorg. Biochem.* **1980**, *12*, 281.
(93) Shamim, A.; Hambright, P.; Williams, R. F. X. *Inorg. Nucl. Chem. Lett.* **1979**, *15*, 243.
(94) Worthington, P.; Hambright, P.; Williams, R. F. X.; Feldman, M. R.; Smith, K. M.; Langry, K. C. *Inorg. Nucl. Chem. Lett.* **1980**, *16*, 441.
(95) Kadish, K. M.; Morrison, M. M. *J. Am. Chem. Soc.* **1976**, *98*, 3326.
(96) Kadish, K. M.; Morrison, M. M. *Inorg. Chem.* **1976**, *15*, 980.
(97) Meot-Ner, M.; Adler, A. D. *J. Am. Chem. Soc.* **1975**, *97*, 5107.
(98) Giraudeau, A.; Callot, H. J.; Jordan, J.; Ezhar, I.; Gross, M. *J. Am. Chem. Soc.* **1979**, *101*, 3857.
(99) Takeuchi, T.; Gray, H. B.; Goddard, W. A., III. *J. Am. Chem. Soc.* **1994**, *116*, 9730.
(100) Sen, A.; Krishnan, V. J. *J. Chem. Soc., Faraday Trans.* **1997**, *93*, 4281.
(101) Autret, M.; Ou, Z.; Antonini, A.; Boschi, T.; Tagliatesta, P.; Kadish, K. M. *J. Chem. Soc., Dalton. Trans.* **1996**, 2793.
(102) Binstead, R. A.; Crossley, M. J.; Hush, N. S. *Inorg. Chem.* **1991**, *30*, 1259.
(103) Hariprasad, G.; Dahal, S.; Maiya, B. G. *J. Chem. Soc., Dalton. Trans.* **1996**, 3429.

(M(IV)/M(III)) oxidation potentials are less affected by substitution of the porphyrin ring.[6,19,37,58,75,99−105] Accordingly, our data show that the ortho isomer is only slightly less sensitive to oxidative degradation than the para and meta analogues (Table 4).

When considered for their ability to facilitate the growth of SOD-deficient *E. coli* (*sodAsodB* strain) in a minimal medium, the ortho isomers of $Mn^{III}TMPyP^{5+}$ and $Mn^{III}TEPyP^{5+}$ were active, while all the iron porphyrins, either cationic or anionic, were not (Figure 4). Addition of 25 μM $Mn^{III}TM\text{-}2\text{-}PyP^{5+}$ and $Mn^{III}TE\text{-}2\text{-}PyP^{5+}$ enhanced the growth of the *sodAsodB* strain also in the richer M9CA medium, whereas all of the isomeric iron porphyrins at 25 μM actually inhibited the growth of this strain (Figure 5). They were also toxic to wild-type *E. coli*. We previously suggested[13a] that the decreased interaction of axially oriented ortho $Mn^{III}TM\text{-}2\text{-}PyP^{5+}$ (and less so of meta $Mn^{III}TM\text{-}3\text{-}PyP^{5+}$) with nucleic acids may account for its diminished toxicity. The same is more true for the bulkier *N*-ethylated analogue.[80] The planar para isomer would be expected to intercalate into DNA.[13a]

The iron porphyrins were found to be toxic to both SOD-deficient (Figure 6A) and wild type *E. coli* (Figure 6B), even under anaerobic conditions. Hence, their toxicity cannot be explained on the basis of reaction with O_2 or species derived from O_2. $Mn^{III}TM\text{-}2\text{-}PyP^{5+}$, which was a growth stimulator for the SOD-deficient strain (*sodAsodB*) under aerobic conditions, had no effect under anaerobic conditions. $Mn^{III}TM\text{-}2\text{-}PyP^{5+}$ had no effect on the growth of the wild-type strain under aerobic or anaerobic conditions, in keeping with its action as an a SOD mimic and relative lack of toxicity. As judged by their behavior in the *E. coli* test system, the Mn porphyrins are preferable to iron compounds as in vivo SOD mimics. The toxicity of the iron porphyrins probably originates from their high affinity for axial ligation,[106,107] whereby they can interfere with protein/enzyme functions. Figure 2 shows that iron porphyrins are prone to axial ligation by 1-methylimidazole while their manganese analogues are not. Iron porphyrins exist in the monohydroxo form in vitro at pH 7.8, given their pK_a values (∼5−7).[19,47,48,60,62,63] Yet in vivo, due to the high cellular protein concentration, they are more likely to be complexed by amino acid residues.

Our data reported here and elsewhere[12,13a] suggest that SOD mimics with $E_{1/2} \sim 300$ mV, i.e. close to the value of the SOD enzyme,[108,109] are preferable because they may be expected to exhibit sufficiently high in vitro SOD-like activity without being dangerously strong oxidants.[110] The β-octabrominated Mn(II) porphyrin $Mn^{II}OBTM\text{-}4\text{-}PyP^{4+}$,[12] as well as β-chlorinated (mono−tetra) derivatives of $Mn^{III}TE\text{-}2\text{-}PyP^{5+}$,[14] appear to be either less efficient or more toxic in vivo[12,111] than the nonhalogenated compounds.

In conclusion, we have shown that although in vitro SOD-like activity is closely related to the metal-centered redox potential and thus also to the pK_a of the porphyrin ligand, additional in vivo factors[13a,80] contribute to the efficacy of compounds intended as SOD mimics. The preference of iron porphyrins for axial ligation makes them toxic and hence not useful SOD mimics. Unfavorable interactions with nucleic acids[13a,80] eliminates the para isomer $Mn^{III}TM\text{-}4\text{-}PyP^{5+}$, leaving the ortho isomers $MnT^{III}M(E)\text{-}2\text{-}PyP^{5+}$ as the best porphyrin-based SOD mimics investigated in our laboratory to date. On the basis of the still significant in vivo SOD-like activity of the meta isomer $Mn^{III}TM\text{-}3\text{-}PyP^{5+}$ shown previously ($E_{1/2} = +0.052$ V vs NHE, 70% of in vivo activity of ortho isomer, $Mn^{III}TM\text{-}2\text{-}PyP^{5+}$),[13a] we propose $E_{1/2} \geq 0.050$ V vs NHE and/or p$K_{a3} \leq 2$ as necessary requirements for the Mn porphyrins to be considered as candidates for in vivo SOD mimics.

Abbreviations: SOD, superoxide dismutase; DMF, *N,N′*-dimethylformamide; ETS, ethyl *p*-toluenesulfonate; 1-MeIm, 1-methylimidazole; TLC, thin-layer chromatography; NHE, normal hydrogen electrode; CV, cyclic voltammetry; M9CA, casamino acid medium; R_f, retention factor, compound to solvent distance ratio; *sodAsodB*, SOD-deficient strain of *E. coli* (JI132*);* wild-type, SOD-proficient, parental strain (AB1157); H_2P, any porphyrin in the form of its metal-free ligand; MP, metalloporphyrin, metal being Fe (FeP) or Mn (MnP); H_2TPP, 5,10,5,20-tetraphenylporphyrin; Me, methyl; Et, ethyl; TMPyP, tetrakis (*N*-methylpyridiniumyl)porphyrin; TSPP, tetrakis(sulfonatophenyl)porphyrin; TCPP, tetrakis(carboxylatophenyl)porphyrin; $H_2T\text{-}2\text{-}PyP$, 5,10,15,20-tetrakis(2-pyridyl)porphyrin. Metal-free ligands (in diprotonated forms), whose iron and manganese complexes are studied in this work: $H_2TE\text{-}2\text{-}PyP^{4+}$ (**1**), 5,10,15,20-tetrakis(*N*-ethylpyridinium-2-yl)porphyrin; $H_2TM\text{-}2(3,4)\text{-}PyP^{4+}$ (**2**, **3**, **4**), 5,10,15,20-tetrakis(*N*-methylpyridinium-2(3,4)-yl)porphyrin (ortho (2), meta (3), and para (4) isomers); $H_2BM\text{-}2\text{-}PyP^{2+}$ (**2a**) 5,10-bis(2-pyridyl)-15,20-bis(*N*-methylpyridinium-2-yl)porphyrin; $H_2TrM\text{-}2\text{-}PyP^{3+}$ (**2b**), 5-(2-pyridyl)-10,15,20-tris(*N*-methylpyridinium-2-yl)porphyrin; $H_2T(TMA)P^{4+}$ (**5**), 5,10,15,20-tetrakis(*N,N,N*-trimethylanilinium-4-yl)porphyrin; $H_2PTr(M\text{-}2\text{-}PyP)^{3+}$ (**6**) 5-phenyl-10,15,20-tris(*N*-methylpyridinium-2-yl)porphyrin; $H_2T(\alpha,\alpha,\alpha,\alpha\text{-}2\text{-}MINP)P^{4+}$ (**7**), 5α,10α,15α,20α-tetrakis(2-methylisonicotinamido)phenyl)porphyrin; $H_2T(TFTMA)P^{4+}$(**8**), 5,10,15,20-tetrakis(2,3,5,6-tetrafluoro-*N,N,N*-trimethylanilinium-4-yl)poprhyrin; H_2TCPP^{4-} (**9**), 5,10,15,20-tetrakis(4-carboxylatophenyl)porphyrin; H_2TSPP^{4-} (**10**), 5,10,15,20-tetrakis(4-sulfonatophenyl)porphyrin; $H_2T(2,6\text{-}Cl_2\text{-}3\text{-}SO_3\text{-}P)P^{4-}$ (**11**), 5,10,15,20-tetrakis(2,6-dichloro-3-sulfonatophenyl)porphyrin; $H_2T(2,4,6\text{-}Me_3\text{-}3,5\text{-}(SO_3)_2\text{-}P)P^{8-}$ (**12**), 5,10,15,20-tetrakis(2,4,6,-trimethyl-3,5-disulfonatophenyl)porphyrin; $H_2T(2,6\text{-}F_2\text{-}3\text{-}SO_3\text{-}P)P^{4-}$ (**13**), 5,10,15,20-tetrakis(2,6-difluoro-3-sulfonatophenyl)porphyrin; $H_2hematoP^{2-}$ (**14**), hematoporphyrin IX. Subscript Mn or Fe was used to denote the metal complex of the particular ligand; H_2TMPyP^{4+}, $Fe^{III}TMPyP^{5+}$, or $Mn^{III}TMPyP^{5+}$ was used when all isomers were being considered.

Acknowledgment. This work was supported in part by grants to I.F. from the NIH, U.S. Army Medical Research Command, the North Carolina Biotechnology Center Collaborative Funding Assistance Program, and Aeolus/Intercardia and to A.L.C. from the NSF and the NIH. P.H. thanks the Howard University CSTEA-NASA Project, Contract NCC S-184, for continual support. We are grateful to Dr. Gerardo Ferrer-Sueta for critically reading the manuscript and to Dr. Stefan I. Liochev for assistance with the *E. coli* experiments.

IC990118K

(104) D'Souza, F.; Zandler, M. E.; Tagliatesta, P.; Ou, Z.; Shao, J.; Van Caemelbecke, E.; Kadish, K. M. *Inorg. Chem*. **1998**, *37*, 4567.
(105) Ghosh, A. *J. Am. Chem. Soc*. **1995**, *117*, 4691.
(106) Scheidt, W. R.; Reed, C. A. *Chem. Rev*. **1981**, *81*, 543.
(107) Morgan, B.; Dolphin, D. *Struct. Bonding* **1987**, *64*, 116.
(108) Lawrence, G. D.; Sawyer, D. T. *Biochemistry* **1979**, *18*, 3045.
(109) Vance, C. K.; Miller, A.-F. *J. Am. Chem. Soc*. **1998**, *120*, 461.
(110) Buettner, G. R. *Arch. Biochem. Biophys*. **1993**, *300*, 535.
(111) Kachadourian, R.; Benov, L.; Batinić-Haberle, I.; Fridovich. I. Unpublished results.